WIND SITE CHARACTERIZATION AND WIND ENERGY POTENTIAL OF MEASUREMENTS AT ISABELA, PUERTO RICO

By

Héctor Alberto Torres Cuevas

A project submitted in partial fulfillment of the requirements for the degree of
Master of Engineering
in
Civil Engineering
University of Puerto Rico, Mayagüez Campus
2013

Approved by

_____	_____
Luis D. Aponte-Bermúdez, Ph.D. President, Graduate Committee	Date
_____	_____
Luis E. Suárez-Colche, Ph.D. Member, Graduate Committee	Date
_____	_____
Iván J. Baiges-Valentín, Ph.D. Member, Graduate Committee	Date
_____	_____
Manuel Toledo, Ph.D. Representative of Graduate Studies Office	Date
_____	_____
Ismael Pagán-Trinidad, MSCE Chairperson of the Department of Civil Engineering and Surveying	Date

Abstract

Electrical energy production is a common concern for society. Conventional energy generation methods rely on chemical processes that use non-renewable resources and can produce dangers byproducts. Renewable energy resources such as Solar power and Eolic energy are becoming of increasing interest. Wind or eolic energy uses the movement of the wind through a rotor system to produce electric current. To assess the potential of eolic energy development, it is necessary to have reliable in situ wind data to understand wind site characteristics and energy potential. The study presented on this report is based on in situ wind data gathered for a period of 1 year, from a meteorological tower located in Isabela, Puerto Rico. The meteorological tower was instrumented with 6 anemometers, two installed at three elevations: 40, 48 and 60 meters, and 2 wind directional vanes installed at 38 and 58 meters in addition to temperature and barometric pressure sensors located at 2 meters from the ground level. The data retrieved from the tower were validated and analyzed to determined wind site characteristics parameters such as the wind shear coefficient (α), turbulence intensity (TI), average wind speed and wind direction. The study also describes the diurnal and nocturnal cycles and its effects on the wind site characteristics and the topography of the surrounding area. From the *in situ* wind data analysis conclusions and recommendations are presented about the wind energy potential.

Resumen

La generación de energía eléctrica es una preocupación común de nuestra sociedad. Métodos de generación de energía convencionales se basan en procesos químicos que utilizan recursos no renovables y pueden producir peligros derivados. Fuentes de energía renovables como la energía solar y la energía eólica son cada vez de mayor interés. Energía del viento o la energía eólica utiliza el movimiento del viento a través de un rotor para producir una corriente eléctrica. Es fundamental tener información precisa para entender las características del viento de un lugar y su potencial para un desarrollo de energía eólica. El estudio presentado en este informe utiliza data de viento recogida durante un período de 1 año, de una torre meteorológica en Isabela, Puerto Rico. La torre meteorológica está equipada con 6 anemómetros, dos instalados en tres alturas: 40, 48 y 60 metros también incluye 2 veletas instaladas en 38 y 58 metros mientras que a 2 metros de la superficie del suelo se encuentran instalados un barómetro y un termómetro. La información recuperada de la torre tales como la coeficiente de fricción o exponente del viento (α), la intensidad de la turbulencia (TI), la velocidad promedio y la dirección promedio del viento se utilizaron para determinar las características del viento para el zona. También se incluyen en el estudio parámetros que afectan las características del viento, como el ciclo diurnos-nocturnos y la topografía de la zona en los alrededores. El análisis resultante se puede utilizar para evaluar el potencial de energía eólica.

Acknowledgment

I would like to thank Dr. Luis Aponte for his support and guidance, and my graduate committee members Dr. Luis Suárez and Dr. Iván Baiges for their contribution to accomplish this project. In addition I would like to thank Aspenall Energies, LLC directors and staff member, I will be forever thankful for the opportunity they have given me and all they have taught me. Special thanks to Eng. Anne Amanda Bangasser and Eng. Vonmare Martínez, their guidance has been greatly appreciated. Dr. Luis Suárez and Dr. Samuel Díaz, I will always be grateful for their inspiration that lead me to the Structural Engineering field. To my many colleagues both academic and professional, thank you, your support has been valuable. Finally, to my family and God, both have been key components in reaching my goals and giving me the strength to do so.

Table of Contents

List of Tables:

List of Figures:

CHAPTER 1. **Introduction**

1.1 Justification

Nowadays one of the greatest struggles of today people development is the need to provide stable, reliable and affordable sources of renewable energy, in order to reduce the high cost of electricity. The current non-renewable methods of energy production, mostly based on fossil fuels, are at high-stake. The chemical process to produce energy from fossil fuels creates toxic byproducts to the environment. Renewable energy generation is becoming more relevant every year in order to reduce the pollution of fossil fuel energy sources and to cut off the dependence. The United States Government has resolved to reduce the greenhouse emissions, and clean renewable energy alternatives are one of the means to achieve this goal. Solar and wind power are becoming two of the major players in the clean energy sector (Securing American Energy | The White House, 2011).

Wind is a renewable energy resource and is essentially free, but in order to determine its potential to produce energy, it requires carrying out a detailed investigation in order to determine the feasibility of the site. Wind-turbines produce electric power, using the wind currents as they pass through the rotor blades. The superstructure consists of four main structural elements: tower, platform, hub, and blades. The structural analysis of a wind turbine involves the understanding of operational wind loads exerted in the superstructure and its entire components. The National Renewable Energy Laboratory (NREL), in collaboration with several groups, has developed various design codes programs to aid engineers in the analysis and design of wind turbines. These codes are widely accepted and accredited as a reliable resource for the analysis of wind turbines. NREL's design codes offer a relatively straightforward method of dealing with the analysis methodology and procedure. Among NREL's codes, *WindMaker* (Laino D., 2005) provides wind profile characteristics, which is representative of a site specific

wind conditions. The wind description information is used in *AeroDyn* (Jonkman J., 2013) and *FAST* (Laino D., 2013) to analyze a proposed wind turbine.

The island of Puerto Rico is no exception to the current global “energy crisis”, in fact, it has real unusual circumstances as it has no current local resources for electrical power generation. The main resources for electrical power generation are petroleum and natural gas (U.S. Energy Information and Administration, 2012). The current position presented by these circumstances highlights the need for renewable and feasible alternatives for energy production in Puerto Rico. The need to describe wind behavior on the complex topography terrain of the Island, in addition, to fulfill reliable structural analysis of wind turbines, are essential factors to assess the alternative of eolic energy on present scenario of the Island.

The University of Puerto Rico at Mayagüez (UPRM) through the Institute of Tropical Energy Environment and Society (ITEAS, for its acronym in Spanish), and in collaboration with Aspenall Energies, are studying the scenario of installing a wind turbine at the UPRM Agricultural Research Facility in Isabela. Aspenall Energies, LLC, a Puerto Rican company dedicated to the development of distributed renewable energy solutions in the Island and the caribbean is in charge of the in situ wind data measurements. In order to determine the feasibility of the Isabela site for eolic energy, the research report aims to address the analysis of the in situ measurements in order to determine the wind site characterization and wind energy potential.

1.2 The objectives of this engineering project are:

- to analyze in situ wind data measurements at the Isabela site provided by Aspenall Energies, LLC,
- to study wind behavior changes and determine parameters needed for the wind site characterization,
- to generate wind speed profiles for the site, and
- to evaluate site potential for eolic energy generation.

1.3 Scope of work

The research project presents data analysis techniques in order to determine the wind site characteristics and energy potential of the proposed site. The work will include the analysis and validation of in situ measurements, a description of the wind profile of the site using the Power Law (α) and determination of the wind energy potential. Also Appendix A presentes an evaluation of NREL's design codes and the benefit it represents in order to have a first assessment of the structural loads of a proposed wind turbine for the site.

CHAPTER 2. Literature review and background

2.1 Wind Engineering – Atmospheric Boundary Layer

The field of wind engineering encompasses a number of disciplines that allow understanding the interaction of wind loads with the natural and built-up man-made environment inside the Atmospheric Boundary Layer (ABL). Among the topics covered in this field as presented by Solari (2007) are:

- wind energy: wind site characterization for Eolic turbines,
- weather: storm forecasting and the mitigation of the resulting damage, and
- meteorology: wind measurement of meteorological phenomena.

In wind engineering understanding the factors that affect the wind's behavior is vital. Understanding the physics and mechanics of the ABL is necessary to comprehend the nature of the air's movement. Factors such as the depth of the boundary layer, roughness of the terrain and latitude location in the earth have a direct effect on the characteristics of the wind. Inside the ABL wind speed increases with height, and wind mean speed vertical profiles (WMSVP) are used to describe the wind speed inside the ABL. A considerable amount of WMSVP models exist, the most commonly employed for meteorological applications is the Logarithmic Law and for engineering applications the Power Law. The Logarithmic Law (Equation 1) has proven to be effective and "has a sound theoretical basis, at least for fully developed wind flow over homogeneous terrain" (Holmes, 2001). To calculate the mean speed at a given height the Logarithmic Law uses a reference height (z), wind shear velocity (u^*), terrain roughness coefficient (z_0), and *von Kármán's constant* (κ) (derived from field study to be around 0.4). These parameters are representative of factors that affect the wind behavior in the ABL. The wind shear represents the change of wind speed or direction with distance; vertical wind shear represents the change of wind with respect to height, a parameter that remains constant along the height of a given site. Roughness length refers to the size of the characteristic eddy (vortex) formed from the friction between the air and the ground surface (Masters, 2004). In the

engineering field, the Logarithmic Law has been found to be difficult mathematically (i.e. negative values for wind speed) and has ideal conditions that are not often achieved. The most currently use WMSVP in engineering is the Power Law (Equation 2), because of its mathematical simplicity and usefulness in relating velocity to elevation. The Power Law has been adopted and widely used in a variety of structural engineering codes around the world like the ASCE 7-05 (2005) in the United States of America and AIJ-RLB (1996) in Japan. It is necessary to note that the power law has no direct theoretical basis; however, there is a correlation of the roughness length used in the logarithmic law and the alpha (α) coefficient of the Power Law (Equation 3). In cases where there are obstructions in the surrounding area, the height used to determine the mean wind speed can be corrected by displacing the WMSVP in the vertical direction (z) an amount equal to the elevation (z_H) of the obstruction; this is known as the zero plane displacement. Figure 2-1 displays this scenario.

Wind shear, mean wind speed profiles equations:

Logarithmic equation

$$u(z) = \frac{u^*}{\kappa} * \log(\frac{z - \ z_H}{z_0}) \tag{1}$$

Power-law equation

$$\left(\frac{u(z)}{u_{ref}}\right) = \left(\frac{z}{z_{ref}}\right)^{\alpha} \quad \text{or} \quad u(z) = u_{ref} * \left(\frac{z}{z_{ref}}\right)^{\alpha} \tag{2}$$

Correlation of power law α coefficient

$$\alpha = \left(\frac{1}{\log\left(\frac{Z_{ref}}{z_o}\right)}\right) \tag{3}$$

where:
- $u(z)$ - average wind speed at z elevation,
- u^* - wind shear speed,
- u_{ref} - wind speed at reference elevation,
- z - elevation at point a,
- Z_{ref} - reference elevation,
- κ - *Von Kármán's constant*,
- α - wind shear coefficient,
- z_0 - roughness length, and
- z_H - zero plain displacement.

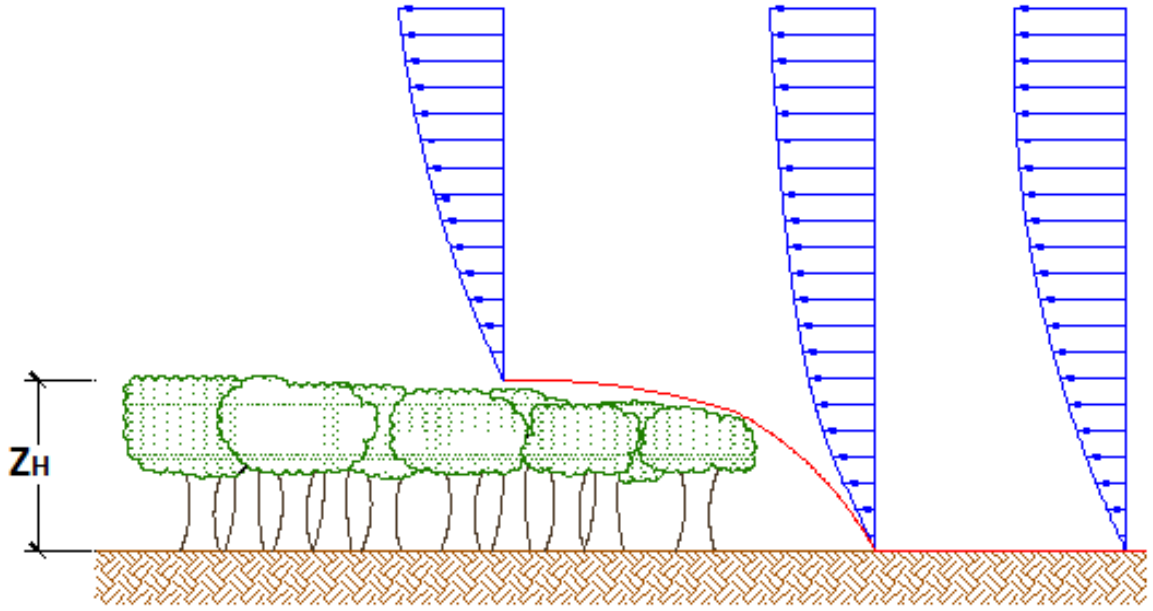

Figure 2-1 : Wind speed profile change due to obstructions

Understanding the nature and behavior of wind involves the representation of how the wind fluctuates in the ABL. Turbulence is present in all wind settings due to the effect of friction between the air movement with the terrain surface. The behavior of turbulence in the wind is complex and highly variable in length and time. Because of the random variability of turbulence it is advantageous to describe it using statistical terms. One of the basic and important statistical factors for the turbulence is the standard deviation of the wind velocity (STD); these deviations can be illustrated for all components of the wind in the Cartesian plane $(x, y, z) or\ (u, v, w)$, respectively referred as the longitudinal, lateral, and vertical components.

An essential factor of the turbulence characteristics is the turbulence intensity or TI (Equation 4) defined as the "ratio of standard deviation of fluctuating wind speed to the mean wind speed" (Rohatgi & Nelson, 1994). The turbulence intensity decreases for higher wind speed conditions, and in lower speed conditions the turbulence intensity increases. In lower wind speeds higher variability is present increasing the value of the standard deviation (σ_i) and producing higher *TI's* where in the higher wind speeds the variation decreases producing lower *TI's*.

Turbulence intensity

$$TI_i = \frac{\sigma_i}{\overline{u_i}} \quad (4)$$

where: $\overline{u_i}$ - mean wind velocity,
σ_i - standard deviation,
i - corresponding wind component (u, v, w),
u - longitudinal wind component,
v - lateral wind component, and
w - vertical wind component.
w - vertical wind component.

The terrain roughness coefficient, and the average sampling time of the measurements, both directly affect the magnitude and behavior of a wind profile. Longer sampling time's generally have wind-speeds of lower magnitude, since it allows more wind fluctuations over time. Typical wind profiles show an increase in wind speed as the elevation increases, the magnitude of the increment is dependent on the terrain exposure location.

2.1.1 Wind data site characterization

The availability of meteorological in situ data for wind site characterization is essential in order to understand the wind behavior and interaction of any immerse body in the ABL. This is even more important in regions prone to extreme meteorological phenomena's such as hurricanes and downburst. Collecting atmospheric data is not always possible, and in most cases studies rely on historical data that do not denote the best site conditions. The data usually available comes from open or suburban terrain exposure (Li & Zhi, 2010) which may differ for a specific site conditions. However, there are methods to manipulating available data to account for differences in terrain exposure conditions and elevation. In situ field measurements are still considered the most reliable source of information, and they present a decisive factor when evaluating wind turbine equipment for a potential site (i.e. matching the specific wind characteristics for a location to the wind turbine manufacturers' specification).

2.1.2 Case Studies

Studies conducted by Li and Zhi (2010) in Beijing, China are essential to better understand the behavior of the ABL and its effects in design conditions. Li's work used a three hundred and fifty meters tower outfitted with approximately thirty anemometers arranged at fifteen elevations in an urban area. Their conclusion presented variations between the calculated parameters of wind shear coefficient, and those specified AIJ-RLB (1996) and the ASCE 7 (2005) standard. This is a significant finding when considering the impact in load calculations.

Singht et al. (2006) had stated that two of the most important components of technical wind data are those related to the performance characteristics of wind turbines and the wind resource assessment. To assess the wind energy potential for a location, several factors have to be taken into consideration such as mean wind speed at a known elevation, wind flow direction and turbulence intensity. It is also important the fluctuation on the wind speed due to seasonal changes and diurnal cycles, which have to be examined to determine optimal conditions for power generation and maintenance. Therefore, the need for in situ meteorological data cannot be overlooked since these measurements provide the most reliable values for the wind resource assessment.

2.2 Motivation: Wind power in Puerto Rico

Wind can be explained as the relative movement of air particles in the ABL of the earth, driven by several forces, especially the solar radiation that produces difference in temperatures and pressure gradient and the Coriolis force generated by the rotation of the earth. The wind energy can be considered as produced by the mass of air as it moves through a mechanical device. Therefore, knowing that power is the rate of energy transfer, a relationship can be established to relate wind speed and power. A wind turbine is a device that transforms the movement of a mass of air through its blades into another form of power, mechanical or electrical, see Figure 2-2 for a diagram of typical horizontal wind turbine.

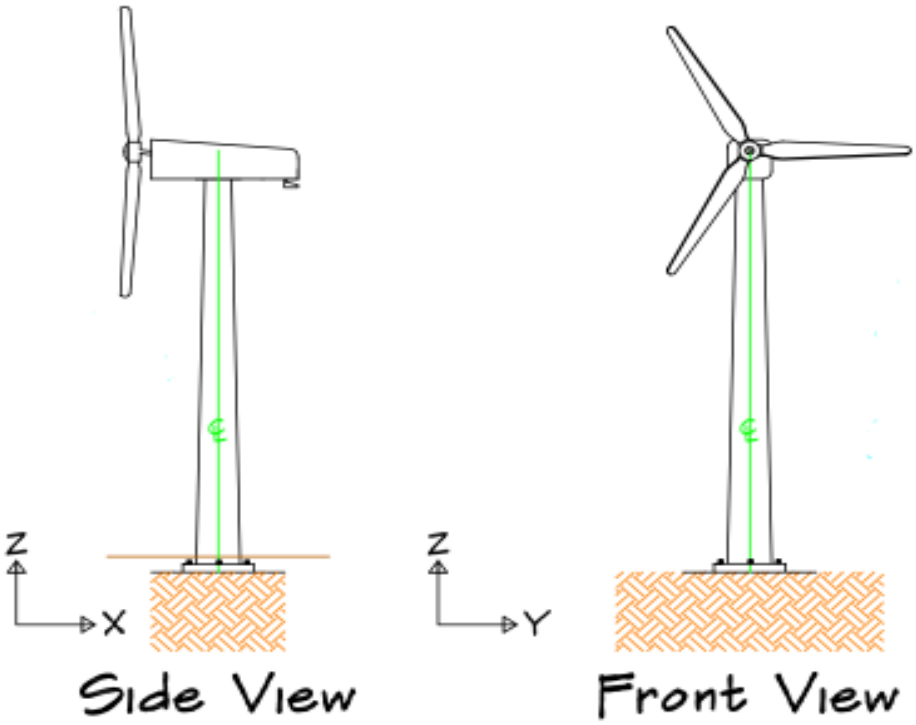

Figure 2-2 : Diagram of typical horizontal wind turbine

Given that the wind velocity is raised to a cubic power on Equation 5 and Equation 6, it is reasonable to conclude that any variation in its magnitude will have a significant effect on the wind power register. In the case of Puerto Rico, there are several map resources from NREL

studies that provide initial information on the wind power for the Island as showed on Figure 2-3. The NREL wind power map shows the wind speed variation along the Island of Puerto Rico using a reference height of 50 meters above ground level.

Wind power

$$P = \frac{1}{2} * \rho * A * u^3 \ (watts) \tag{5}$$

Wind power potential

$$\frac{P}{A} = \frac{1}{2} * \rho * u^3 \ (\frac{watts}{m^2}) \tag{6}$$

where: u - Wind velocity,
A - Projected sweep area by blades, and
ρ - Air density.

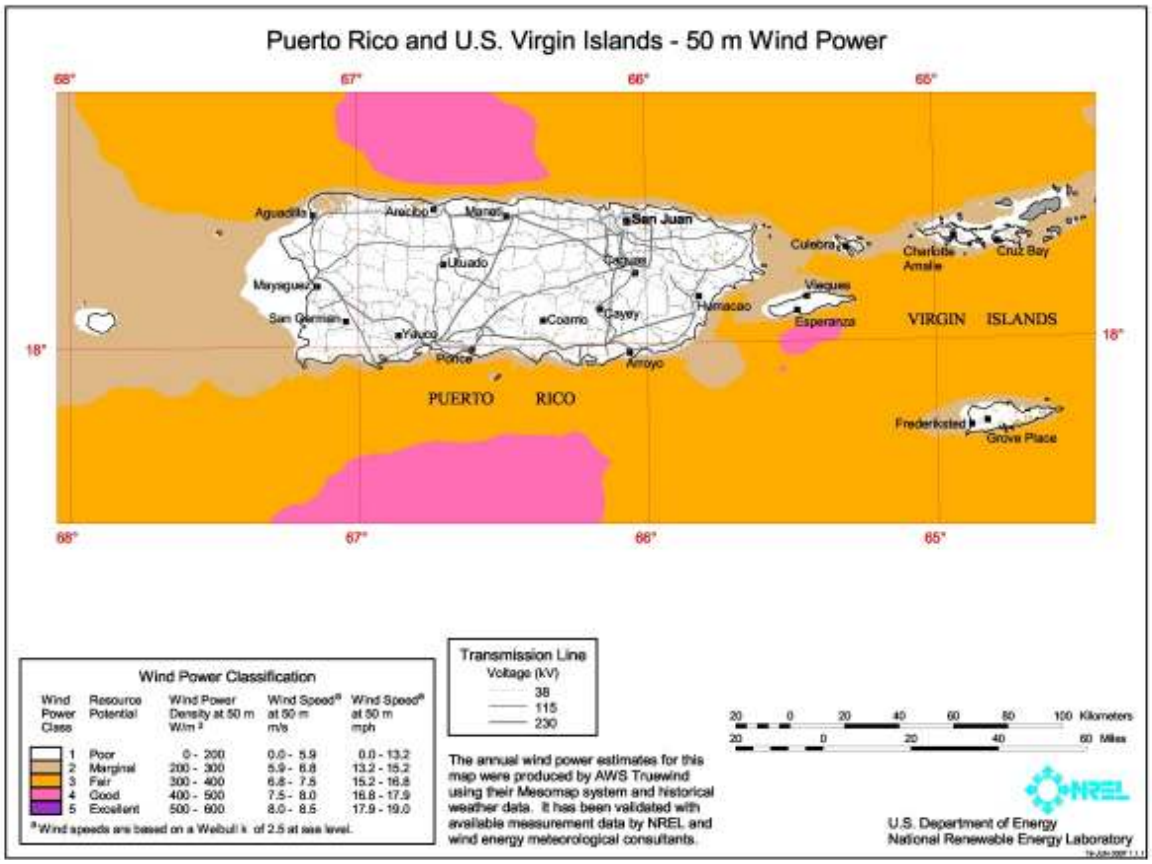

Figure 2-3 : Puerto Rico and U.S. Virgin Island – 50m above ground level Wind Power map from NREL

In the article by Altaii and Farrugia (2003) a study was conducted in Puerto Rico at four sites in Aguadilla, Ponce, Gurabo, and San Juan. The data were collected from May 1998 to June 2000, for the purpose of wind characterization at each site. The study reveals that there are “reasonable wind conditions” for wind energy generation. Their work presents an initial idea of the direction and magnitude of the expected mean wind speed in these locations in Puerto Rico, and it can be used to get a more refined assessment of the wind energy resource. The data can be used to determine preliminary potential for a wind turbine site; however, it is still recommended to collect in situ data in order to have a more reliable scenario for the potential sites.

CHAPTER 3. **Met-Tower wind data**

3.1 Isabela in situ data

In this study case, wind data was collected from a meteorological tower installed by Aspenall Energies, LLC. The tower installation was part of a collaborative effort between the University of Puerto Rico at Mayagüez and Aspenall Energies, as part of a wind resource assessment research to characterize the wind condition of the site. The research long term goal is to install a prototype wind turbine. The meteorological tower (Met-Tower) was located at the Isabela Agricultural Research Station of the University of Puerto Rico at Mayagüez (see Figure 3.1) at latitude 18°28'07"N and longitude of 67°02'23"W.

(a) (b)

Figure 3-1 : Aspenall Isabela, PR Met-Tower

(a) Aerial Image (Google Earth, 2009) (b) Site Photo,

The surrounding area of the Met-Tower site consist of terrain exposure combination of sub-urban terrain to the east and a more open terrain that belongs to the facilities of the agricultural station to the west. There were several trees located in the perimeter of the agricultural station and they range in elevation from one meter to around ten meters. The trees created a low density line around the perimeter.

The tower was manufactured by *Second Wind* Company (Second Wind Systems Inc., 2013) and it consists of a sixty meter tilt up tower. The main structure composed of a set of painted galvanized steel cylinders with a diameter of 165 millimeter (6.5 inches) at the top of the tower and 222 millimeter (8.7 inches) at the bottom part. The support system consisted of a set of guyed cables connected to the tower and a set of fixed anchors to the ground. Figure 3.2 presents a diagram of the tower showing the instrumentation location. The instrumentation arrangement consisted of six *NRG# 40C* three-cup anemometers, distributed in three locations in the tower at 60, 48 and 40 meters. In addition to the anemometer there are two *NRG #200P wind direction vanes* located at fifty eight meters and thirty eight meters. The anemometers were arranged at sixty degrees each from the main wind direction (120 degrees between them), and the wind vanes where placed directly in the north direction. In addition to the wind data instruments, sensors for temperature and pressure, an *NRG #110S temperature sensor,* installed set at two meters from the ground level.

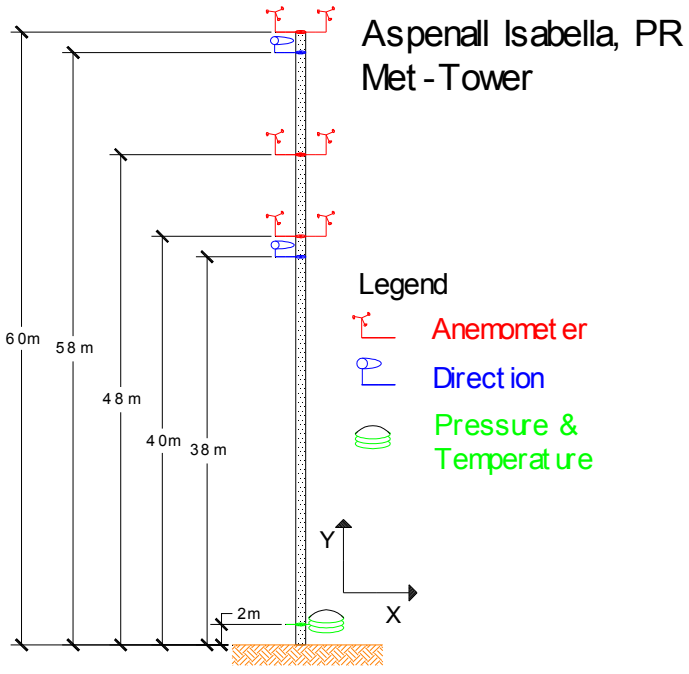

Figure 3-2 : Diagram of measurement tower in Isabela, Puerto Rico

The data collected were presented in an arrangement of channels (CH), after processing the raw data files with the *Symphony Data Retriever* program, provided by *NRG Systems* (2012). The data retrieved from the Met-Tower delivered information about wind speed, wind direction, barometric pressure, and air temperature at ten minutes and hourly averages intervals. The channels numbered from one to fifteen included an array that incorporates minimum, maximum, average, and standard deviation values for each measured data record. In addition to the data channels, each record included its corresponding time stamp. Once the data had been collected and stored (as an ASCII file), it was analyzed using various softwares such as MATLAB®, Microsoft Excel®, and Wind Rose Plots for Meteorological Data (WRPLOT View™). Table 3.1 presents a description of the data stored by each channel, units of measurement, and location of the measurement instrument.

Table 3-1 : Description of data channels from Aspenall Energy, LLC Isabela Met-Tower

Record Channel ID & Time Stamp	Instrument Elevation (m)	Description	Measurement unit
"Date & Time Stamp"		String number	month/day/year hh:mm:ss
1	60	Wind Velocity	$m \cdot s^{-1}$
2	60	Wind Velocity	$m \cdot s^{-1}$
3	48	Wind Velocity	$m \cdot s^{-1}$
4	N/A	N/A	N/A
5	N/A	N/A	N/A
6	N/A	N/A	N/A
7	58	Wind direction	degrees
8	38	Wind direction	degrees
9	2	Temperature	°C
10	2	Pressure	mbar
11	N/A	N/A	N/A
12	N/A	N/A	N/A
13	48	Wind velocity	$m \cdot s^{-1}$
14	40	Wind velocity	$m \cdot s^{-1}$
15	40	Wind velocity	$m \cdot s^{-1}$

** N/A – not applicable, empty channel

3.2 Data validation

Once the data had been processed, the first step involved the validation of each channel in order to account for any abnormal readings and/or missing records. The Isabela Met-Tower was commissioned on March 30, 2011 and the data used in this research incorporates one year

of data from the commissioning date to March 31, 2012. The yearly data set provides an overview of the seasonal variations of wind, prevailing wind conditions, and extreme events.

The data of CH 01 was found to have faulty records for most of the study period due to physical damage in one of the anemometers located at sixty meters. For several months (March 30, 2011 to June 8, 2011) the temperature and pressure data was faulty. With regard to the wind vane data on direction, both CH 07 and CH 08 had a shift in the recorded data of 180 degrees until June 08, 2011 09:40. Taking into consideration these factors, the analysis of the remaining data records was properly conducted.

A useful tool in the validation of data was the graphical display of the records. Figure 3-3 shows the behavior of the annual wind speed variation in a time series format for CH 03 located at 48 meters from ground level from April 2011 to April 2012.

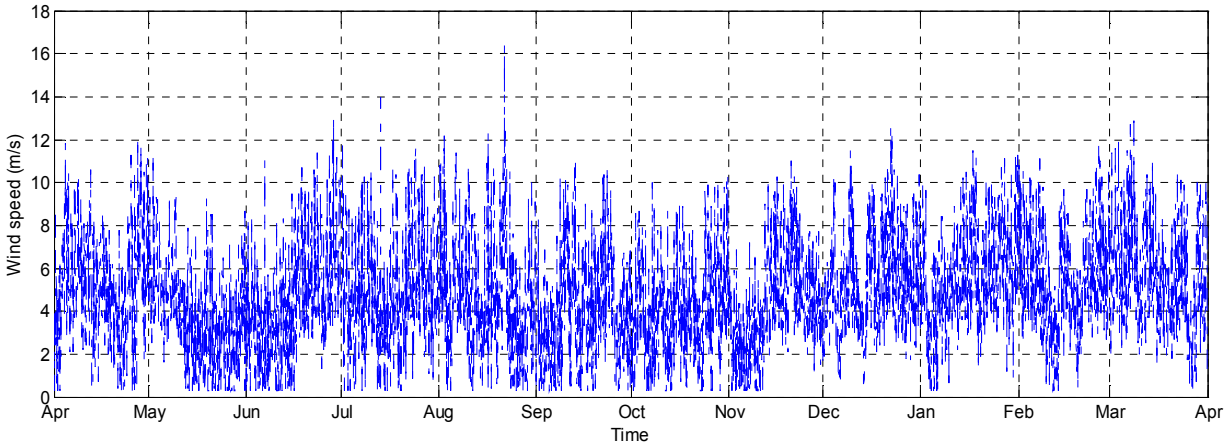

Figure 3-3 : Channel 03 wind speed annual time series (Apr 2011 – Apr 2012)

Figure 3-4 compares the wind speed data for a 3 month period from April 2011 through June 2011 between anemometers at 60 meters (CH 02) and 40 meters (CH 15), similar patterns are observed denoting similarity in the wind behavior at these two vertical locations. The main difference in the pattern is the magnitude that, as expected, has greater magnitudes at higher elevation. The correlation coefficient “R” for the two elevations is 0.983 meaning that as it is close to 1.0 the two values are positively correlated, as one increases the other will have a similar behavior.

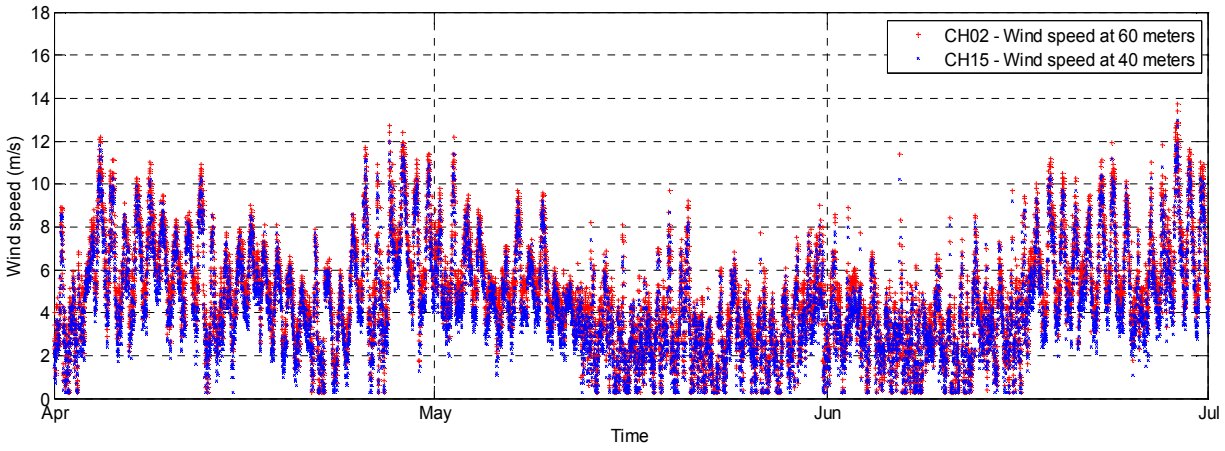

Figure 3-4 : Wind speed time series at 60 m (CH 02) and 40 m (CH 15) for the period of June 2011 thru July 2011, R = 0.98

The data from the two wind directional vanes, CH07 at 58 meter and CH08 at 38 meters are compared in Figure 3.5 and 3.6. Both figures present a plot of the wind direction data for the entire record applying cosine and sine function respectively, the x-axis in the data for CH08 and the y-axis been data from CH07. The cosine and sine functions are used to maintain consistency in the data when the directions are 360° or 0°. For both cases the linearization of the graph have an intercept close to 0 (< 0.03 variation) and a slope of close to 1 (< 0.03 variation). By using this information we can reasonably say that both directions have a good correlation. The results obtained from the linearization have a coefficient of determination "R^2" close to 0.9. Given the fact that a value of 1 refers to a linearization having a perfect fit and 0 not been representative at all, the results obtained are considered trustworthy.

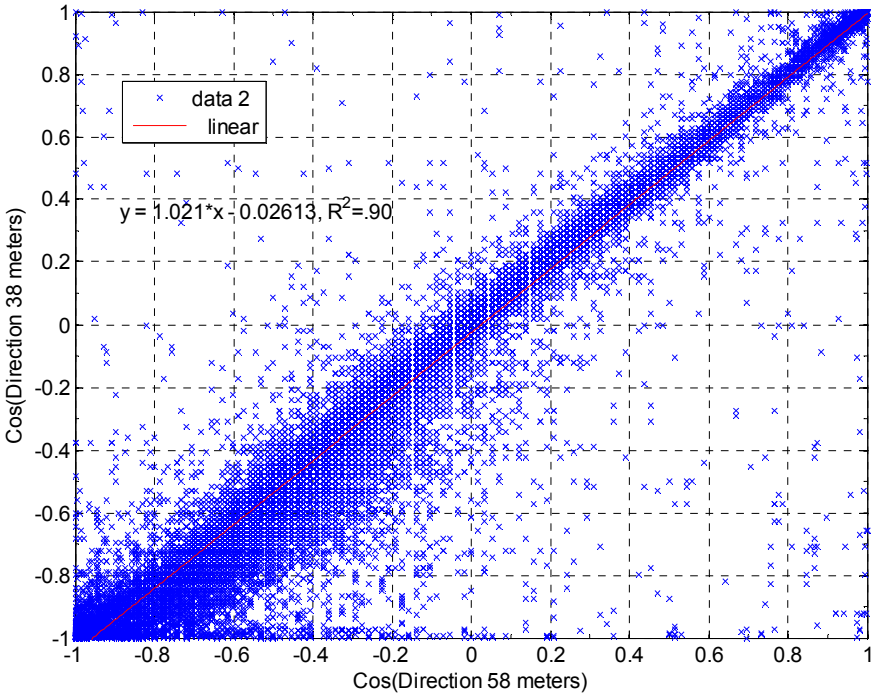

Figure 3-5 : Cosine of wind direction at 38m (CH 08) vs. 58 m (CH 07)

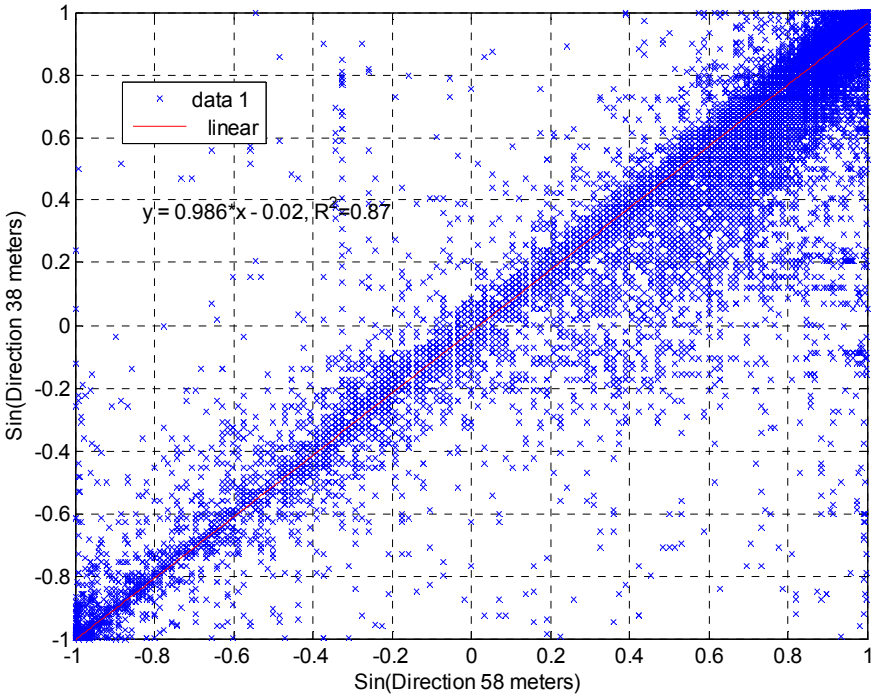

Figure 3-6 : Sine of wind direction at 38m (CH 08) vs. 58 m (CH 07)

3.3 Wind analysis

In the analysis a distinction was made in the data used to calculate the different parameters as part of the in situ wind site characterization. The cut-in wind speed is the minimum speed at which the wind turbine will generate usable power to be storage; it is in the range of three to four meters per second. Therefore for this study a minimum wind speed threshold at the elevation of sixty meters was determined to be 3.0 $m \cdot s^{-1}$. Table 3.2 presents the total number of ten minute records used for the study time frame and those that were dropped out (time frames will be explained in section 3.3.2). In addition Table 3.2 indicates that 17% of all records were dropout and that the majority of the dropout records were in the nighttime where the expected wind speeds are lower in magnitude.

Table 3-2 : Ten minute records used (Apr-2011 to Apr-2012)

Condition	Records above wind speed threshold of 3 m·s-1 @ 60m	Total number of records	Discarded records
Day	22949	26483	13%
Night	21205	26454	20%
All Data	44154	52937	17%

3.3.1 Variations

Wind, like all natural phenomena, is created and affected by a number of factors that induce variability in its behavior. Some of the most significant factors are change in temperature during diurnal and nocturnal cycles, change in seasonal periods of the year, and change in surrounding surface conditions (i.e., topographic effects and built-up environment) along the wind's path. For a specific location, the behavior of the wind will then vary as the topographical conditions in each direction change.

3.3.2 Day-Night

The thermal change that occurs as solar radiation rise the temperature in the earth's surface from night to day changes the characteristics of the wind (i.e., wind speed and direction). A

swing can be perceived for wind speed as peaks and valleys in a time series plot such as in Figure 3-7.

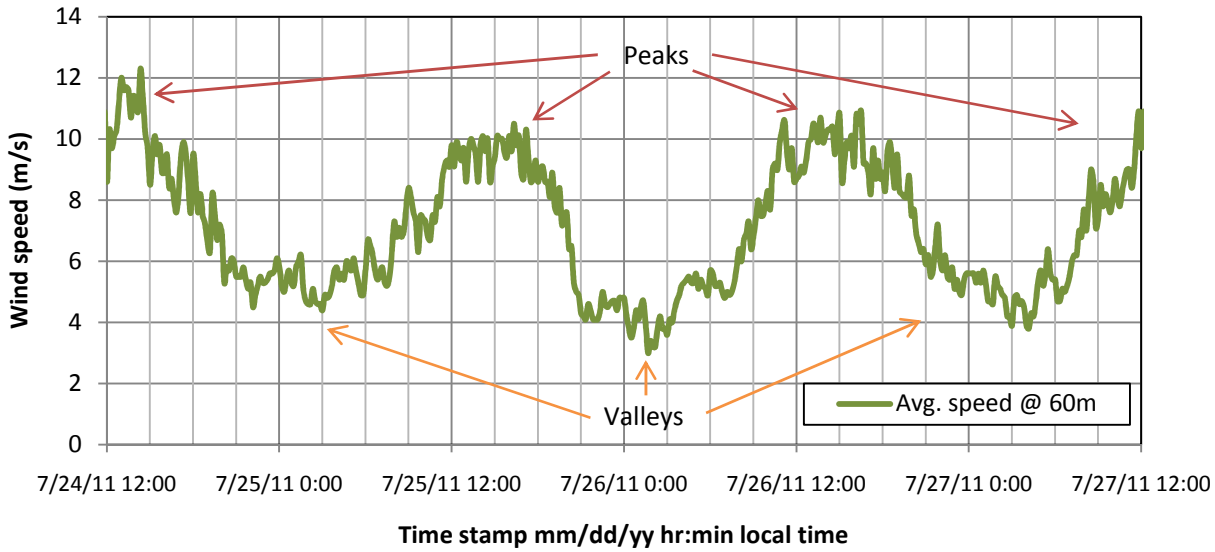

Figure 3-7 : Behavior of wind speed for a 3 day period

A three day sample of the wind speed was chosen to better display the diurnal and nocturnal wind cycles. The wind speeds are presented in Figure 3-7 for the three day sample, peaks show the daytime increase in temperature that heat up the air that moves upward to cool down away from the heat at ground level. The wind will also be affected by the difference in temperature that occurs between the ground surface and the surface of the water. In the daytime the ground surface will have higher temperature and the surface of the water will be cooler, because of the difference in pressure the temperature creates the wind in the daytime will move from the ocean to the cost and *vice versa* in the nighttime (Morell, et al., 2012). The effect of the daytime and nighttime cycles on direction will be presented in section 3.3.4.

In Figure 3-8 is displayed for their specific hour of the day the average wind speeds at 60 meters height for the study period (April 30, 2011 to April 30, 2012) , the square markers indicate the average wind speed for the respective hour. To understand the range of variability of each hour, two standard deviations above (Upper bound-diamond markers) and below (Lower bound-triangular markers) are displayed around the average. At the Isabela Met-Tower site the diurnal wind cycle behavior from 6:00 AM to 8:00 AM changes from lower magnitude to

higher magnitude and from 6:00 PM to 8:00 PM swap once more from higher to lower magnitudes. For the purpose of the analysis conducted, “Day” or “daytime” refers to the wind data recorded between 7:00 AM to 7:00 PM, and “Night” or “nighttime” refers to the data recorded during the remaining time. The reference hours were chosen to capture the change in the diurnal and nocturnal daily cycles of the prevailing winds generated by sea and land breezes respectively. In order to compare directly the results from the analysis, the same number of hours for the daytime and nighttime were used.

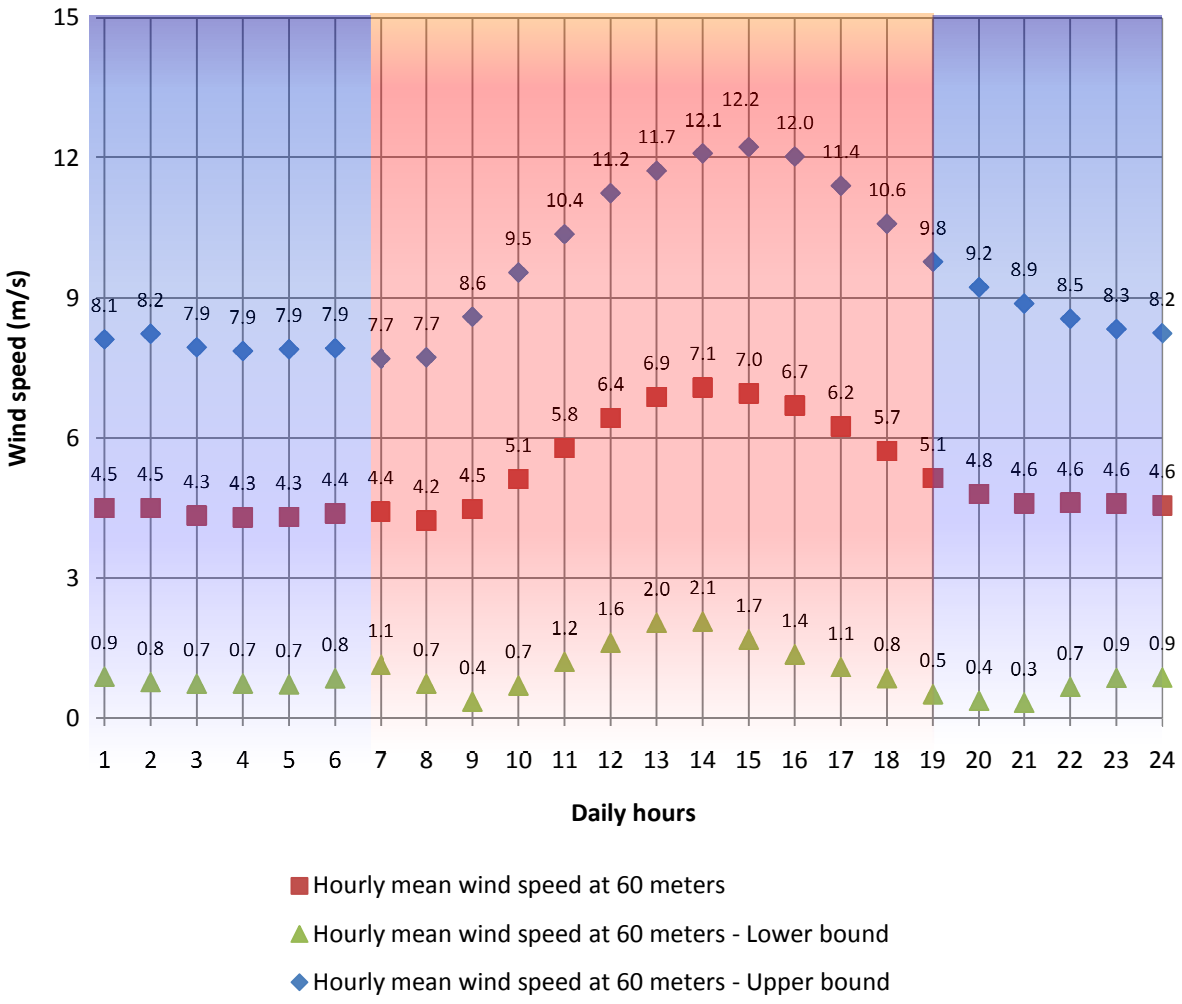

Figure 3-8 : Hourly variation of wind speed in a 24 hour period

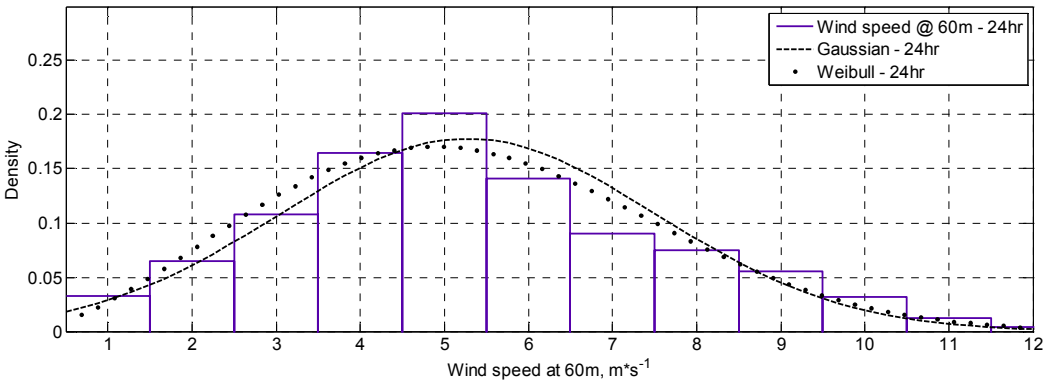

Figure 3-9 : Histogram of all Wind speed (at 60m) distribution from (Apr-2011 through Apr-2012)

A frequency distribution of the wind speed provides a graphical measure of how the wind behaves and how the wind speed magnitudes are distributed. Figures 3-9 and 3-10 show a histogram of the frequency of different 10 minutes wind speeds segments at 1 $m \cdot s^{-1}$ intervals from 0.5 to 12 $m \cdot s^{-1}$ covering 97 % off all data. The data above 12 $m \cdot s^{-1}$ is less than 0.5 %, while the data below 0.5 $m \cdot s^{-1}$ incorporates the anemometer low wind speed threshold where it initializes (minimal readings of the anemometer are 0.3 and 0.4 $m \cdot s^{-1}$). A Gaussian distribution fits well a frequency distribution of the mean wind speed at 60 meters collected during the study period as presented in Figure 3-9 (not applying threshold) while the Weibull has a similar fit and is the most widely use fit for wind speed distribution and energy calculations (Lo Brano, et al., 2001).

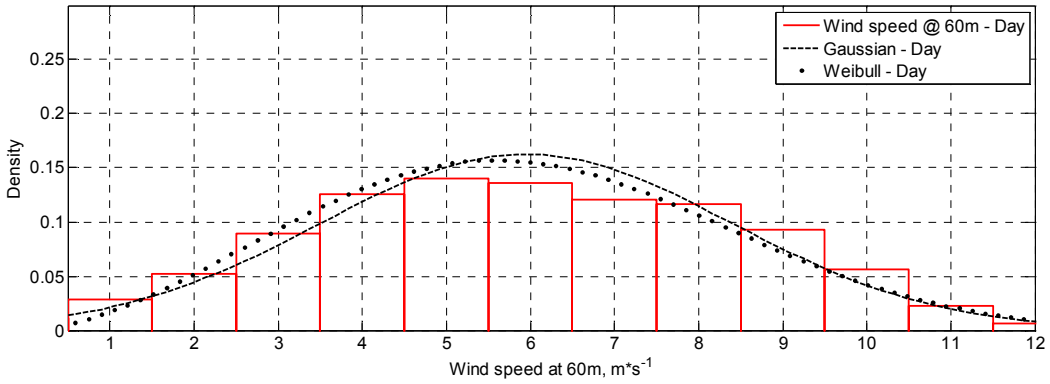

(a)

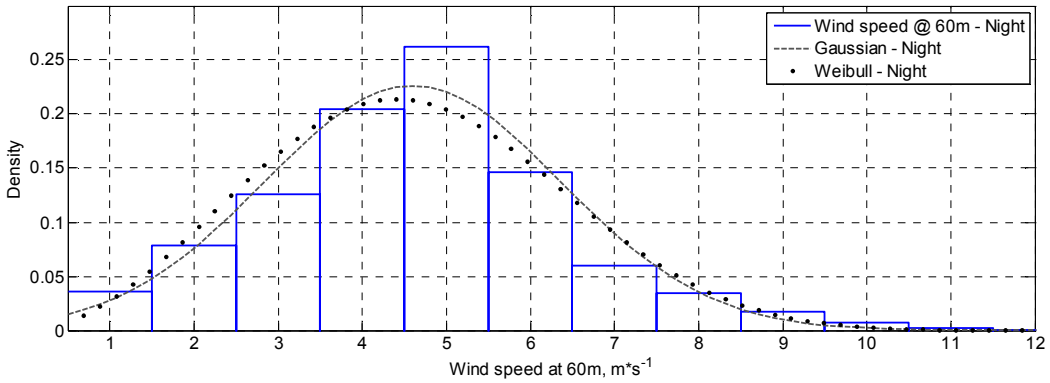

(b)

Figure 3-10 : (a) Daytime and (b) nighttime histograms of wind speed (at 60 m) distribution from (Apr-2011 through Apr-2012)

Equations 7 to 8 present the equations that govern the Gaussian and Weibull Probability Density Function (PDF). The Gaussian or Normal PDF uses the variance and standard deviation to create a pattern or fit that represents the behavior of a sample, it is the initial approach for most data fittings. The Weibull PDF is a widely use in wind energy applications. The fit relays on the determination of shape "*k*" and "*c*" scale parameters, usually determent in an interactive process,

Gaussian probability distribution function - GPDF

$$f_x(x) = \left(\frac{1}{\sqrt{2 * \pi} * \sigma_x}\right) * e^{\left[\frac{-(x-\overline{\overline{X}})^2}{2*\sigma_x^2}\right]} \quad (7)$$

Weibull probability distribution function -WPDF

$$f_x(x) = \left(\frac{k * x^{k-1}}{c^k}\right) * e^{-\left(\frac{x}{c}\right)^k}$$

$$k = \left[\frac{\frac{1}{N}\sum_{i=1}^{N} x_i^{\propto} \ln x_i}{\sum_{i=1}^{N} x_i^{\propto}} + \frac{1}{N}\sum_{i=1}^{N} \ln x_i\right]^{-1} \quad (8)$$

$$c = \left(\frac{1}{N}\sum_{i=1}^{N} x_i^{\propto}\right)^{\frac{1}{\alpha}}$$

where:
- N = Number of samples,
- σ_x = standard deviation of the sample (S.D.),
- σ_x^2 = variance of the sample,
- x = sample data,
- $\bar{X}$ = sample mean,
- k = shape parameter (dimensionless) and
- c = scale parameter (see (Lo Brano, et al., 2001))

When the wind speed distribution is separated for daytime and nighttime as indicated in Figure 3-10a and 3-10b respectively, there was a considerable change in the shape of the individual distributions, but both showed Gaussian behavior. For daytime, wind speed distribution was spread out over a wider range (around 3 to 9 0.1 $m \cdot s^{-1}$), and in nighttime the values were concentrated in a smaller range (around 2.5 to 6 0.1 $m \cdot s^{-1}$). Table 3-3 presents the statistical data parameters such as average, Standard Deviation (SD), distribution around the mean of the frequency distribution or Skewness for GPDF (Equation 9) and the concentration of values on the center or the form of the peak in center know as Kurtosis for the GPDF (Equation 10).

Skewness

$$s_x = \left(\frac{1}{N * \sigma_x^3}\right) * \sum_{i=1}^{N} (x_i - \bar{X})^3 \quad (9)$$

Kurtosis

$$\mu_4 = \left(\left(\frac{1}{N * \sigma_x^4}\right) * \sum_{i=1}^{N} (x_i - \bar{X})^4\right) - 3 \quad (10)$$

Table 3-3 : Statistical behavior for each time period at 60 meters

	Units	24hr	Daytime	Nighttime
Average, $\bar{X}$	m·s^{-1}	5.19	5.89	4.49
SD, σ_x	m·s^{-1}	2.35	2.55	1.89
Skewness. s_x	m·s^{-1}	0.30	0.02	0.20
Kurtosis, μ_4	m·s^{-1}	-0.14	-0.61	0.68
Scale parameter, c	m·s^{-1}	5.84	6.62	5.03
Shape parameter, k	N/A	2.31	2.45	2.48

For the daytime the average wind speed has a higher magnitude than the other time frames (5.89 m·s^{-1}), as expected during the diurnal wind cycle. The daytime also presents higher SD (2.55 m·s^{-1}) meaning it is more distributed along the values and because of the lower Skewness (0.02) the distribution is relatively symmetrical around the mean. The negative low magnitude Kurtosis for the day (-0.61) presents a distribution that has a lower peak than a normal distribution and that denote a more even distribution along the wind speeds range. In contrast the nighttime has the lowest average wind speed lowest in magnitude of the time frames (4.49 m·s^{-1}) with a concentrated distribution around that value. The low values of SD (1.89 m·s^{-1}), the higher positive Kurtosis (0.68) and a higher the daytime Skewness of (0.2) match a localize distribution about the mean value. The statistical parameters for the entire dataset fall in between both the nighttime and daytime wind cycles, having an average wind speed of 5.19 m·s^{-1} with a SD of 2.5 m·s^{-1} and Skewness and Kurtosis of 0.3 and -0.14 respectively. The parameters c and k for the Weibull PDF produced similar fit as parameter of

the Normal PDF. Daytime scale parameter c is the highest in magnitude having 6.62 that produce a wider distribution then the others (Nighttime the lowest 5.03 and All data 5.84. Shape parameter *k* has the highest magnitude is in the Nighttime 2.48 $m \cdot s^{-1}$ that produce a higher bell distribution then the others (Daytime 2.45 $m \cdot s^{-1}$ and the lowest at 24hr 2.31 $m \cdot s^{-1}$). The effect on wind direction in the daytime and nighttime are presented in section 3.3.4.

3.3.3 Hurricane season

As defined by the National Oceanic and Atmospheric Administration (NOAA) and the National Hurricane Center (NHC), the hurricane season for the Atlantic basin starts on June 1st and ends on November 30th. A hurricane can be defined as a moving mass of air rotating around a clear center structure, called the eye, with a radius of several kilometers. Hurricane intensity can and is categorized by the Saffir-Simpson Hurricane Wind Scale (SSHWS) based on the intensity of sustained winds at ten meters over open water exposure. Table 3-4 shows the wind speed range of hurricane categories as defined by the SSHWS and modified by NOAA in 2012 to widen the range of sustained wind speeds that fall under the fourth category from 131 - 155 mph to 130 - 156 mph (Schott, et al., 2012)

Table 3-4 : Saffir-Simpson Hurricane Wind Scale

Category	Wind speed (mph) at 10 meter height over water	
	Sustained wind	3 sec wind gust
I	74 - 95	94 - 121
II	96 - 110	122 - 140
III	111 - 129	141 - 165
IV	130 - 156	166 - 197
V	> 157	> 198

During August 22 to 23, 2011 Hurricane Irene passed along the area of Puerto Rico. It was categorized as a category I Hurricane in the SSHWS scale. Figure 3-11 presents the time history of the wind speed at 60 meters and direction at 58 meters during Irene. The plot has two y-axis; the left y axis refers to the blue line trace which indicates the 10 minute average wind

speed at the 60 meter height in $m \cdot s^{-1}$ and the right y axis refers to the red dot trace which indicates the wind direction in degrees. During the event the maximum recorded 10 minute average wind speed at 60 meter height was 17.3 $m \cdot s^{-1}$ @ 76° (North-East) on August 21, 2011 23:30 local time. It is important to note that at hub height over sixty meters the maximum wind speed experienced by a turbine will be higher than the observed wind speed at 60 meter. The design wind speed in Puerto Rico as defined in the ASCE-7-05 (2005) is 145 mph (65 $m \cdot s^{-1}$) which is for a 3 second wind gust measured at 10 meter from the ground for a terrain exposure z_0 = 0.02 m. This speed corresponds to a Category 3 Hurricane as defined by the SSHWS.

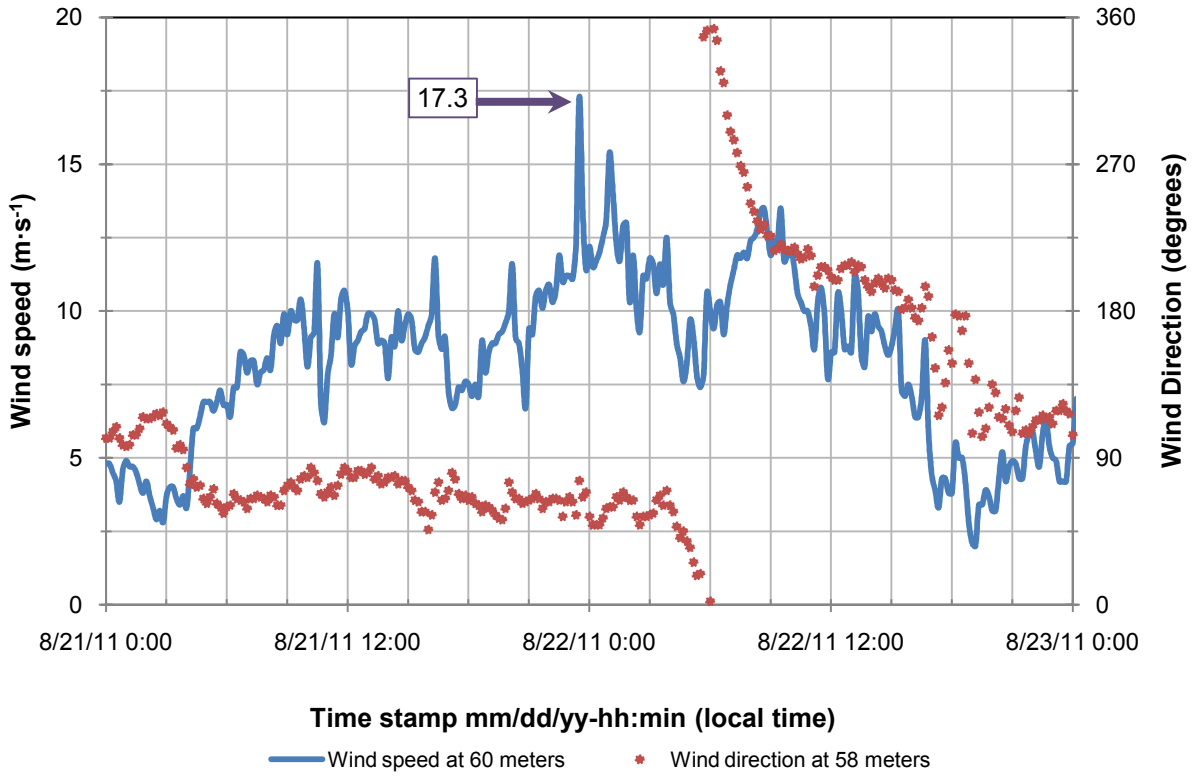

Figure 3-11 : Wind measurements during the passage of Hurricane Irene 2011

3.3.4 Directional wind effects

Wind is affected by the upwind ground surface roughness it travels causing a significant effect on its behavior, based on topography features (i.e., isolated hills, ridges, and escarpments), vegetation and constructed facilities (i.e., buildings, houses, etc.). The wind

movement through topographic features speeds-up the wind as it adjusts to pass over; this creates a speed adjustment in the wind profile. Figure 3-12 illustrates the speed-up effect as wind flows over a hill. It can be noted that while it reaches the crest of hill the wind speed increases as the mass of the moving air higher elevation is combined with the mass of air displaced by the topographic feature, once it passes the crest of the hill the wind profile recoils and the wind speed decreases. A smoother surface like the one present in open land is associated with lower roughness length (z_0) and lower shear coefficient (α), meaning a more uniform wind flow with less turbulence. Urban areas or where there are higher variations in the topographical features and vegetation are related to higher roughness length and wind shear values.

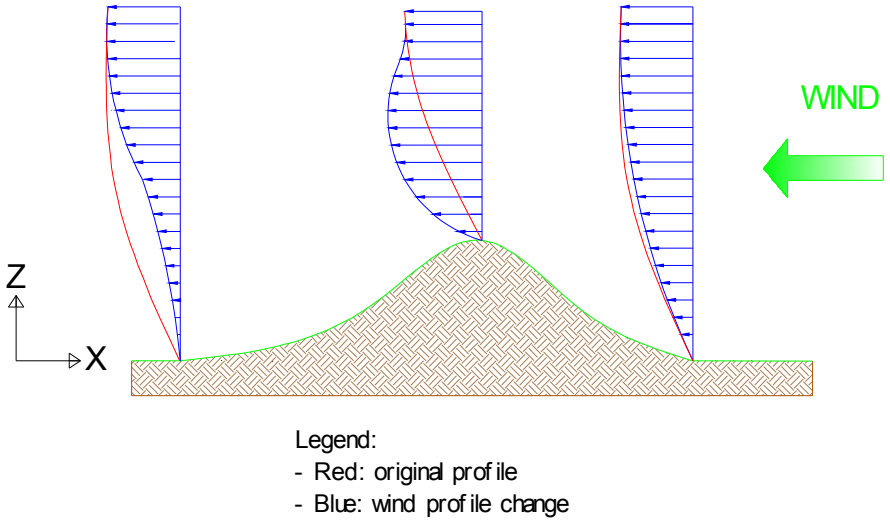

Figure 3-12 : Speed-up effect on wind profile over a hill

In ASCE 7 (2005) the extent of the terrain that has an effect on a structure is primarily defined by two factors; the shape of topographic features and the terrain roughness, where the latter is mainly the vegetation and constructed facilities in the upwind wind direction up to two miles for open terrain site. In order to characterize the terrain's effects this study examines the variation in a 2.0 mile (3.2 km) radius as illustrated in Figure 3-13. The figure displays an aerial view, the image was retrieved from *Google Earth* (Google Earth, 2009), with the Met-Tower located in the center. There are eight lines representing the eight cardinal directions set out up

to the diameter of the outermost circle. The North-West-South area (left side) that surrounds the Met-Tower has a combination of some scattered low rise structures (less than 12 ft tall) but are mostly open farmland. The remaining directions the North-East-South area (right side) have a higher density of low rise structures and small vegetation (less than 12 ft tall).

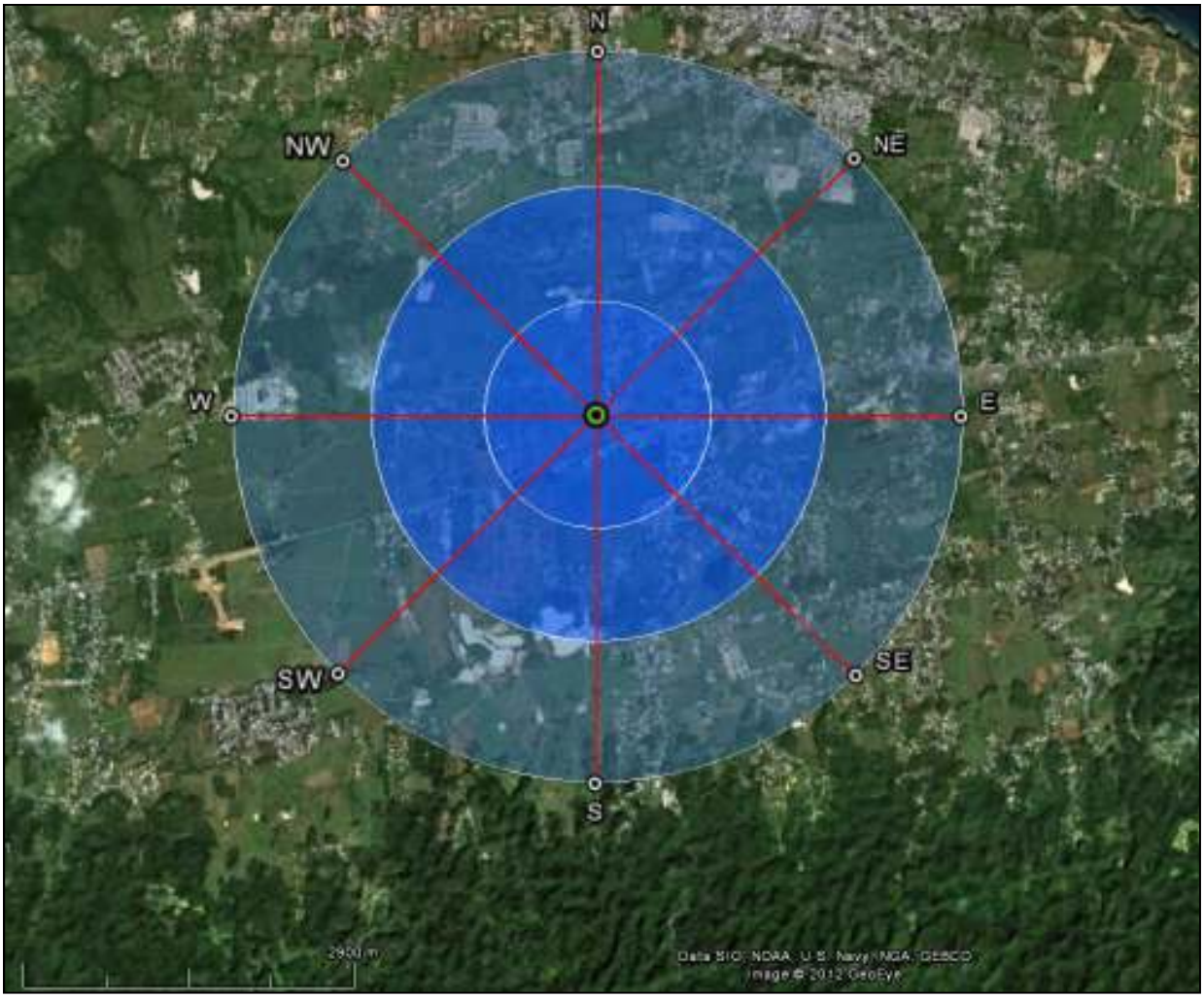

Figure 3-13 : Topographical layout for Met-tower

Topographical profiles have been created using the information found in *Google Earth* as a initial look for the terrain conditions. The profiles are configured to cover a two mile length (x-axis) beginning at the tower location and covering 60 to 200 meters of elevation from sea level (y-axis). When the topographical profiles are examined the east and west directions (Figure 3-14 and 3-15) have only around twenty meters in variation in each direction, and thus the topography effect is not as predominant in these directions. Figure 3-16 and 3-17 show the

elevation profiles for the North and South upwind direction. These have higher variations than the East and West, up to eighty meters. The topographical effects in these directions are more pronounced and the wind's behavior becomes less uniform and more turbulent. The North profile displays an abrupt change in elevation from 120 meter to 140 meters at 0.5 mile and then a progressive decrease in elevation from 1 mile until leveling at an average of 80 meters for the rest of the profile. In the South profile there is a progressive increase in elevation starting at 120 meters and ending at 200 meters about 2 miles from the tower. The slope however is not constant and there are points where for small intervals (less than 0.5 miles) the elevation decreases and then increases rapidly. The more abrupt the changes in topography, the higher the mechanical turbulence it creates in the wind's behavior producing higher turbulence intensities and wind shear coefficients.

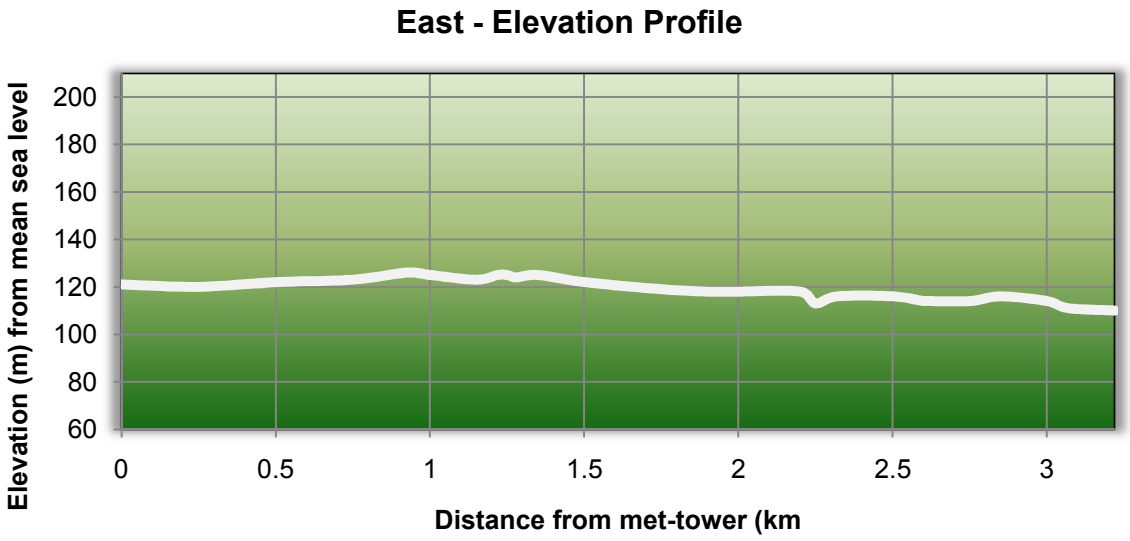

Figure 3-14 : East direction elevation profile for 3.3 km from the Met-tower

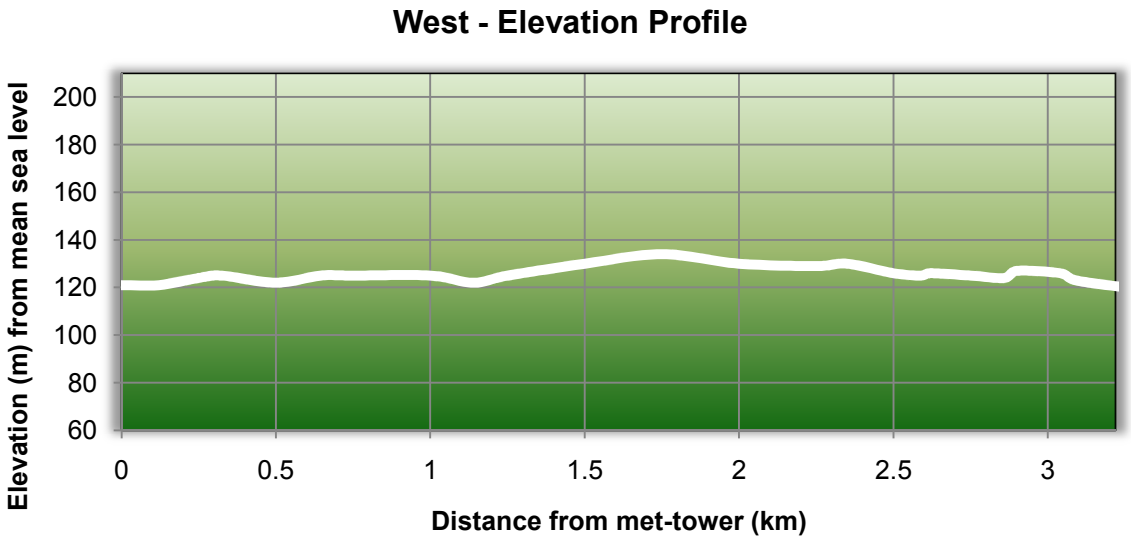

Figure 3-15 : West direction elevation profile for 3.3 km from the Met-tower

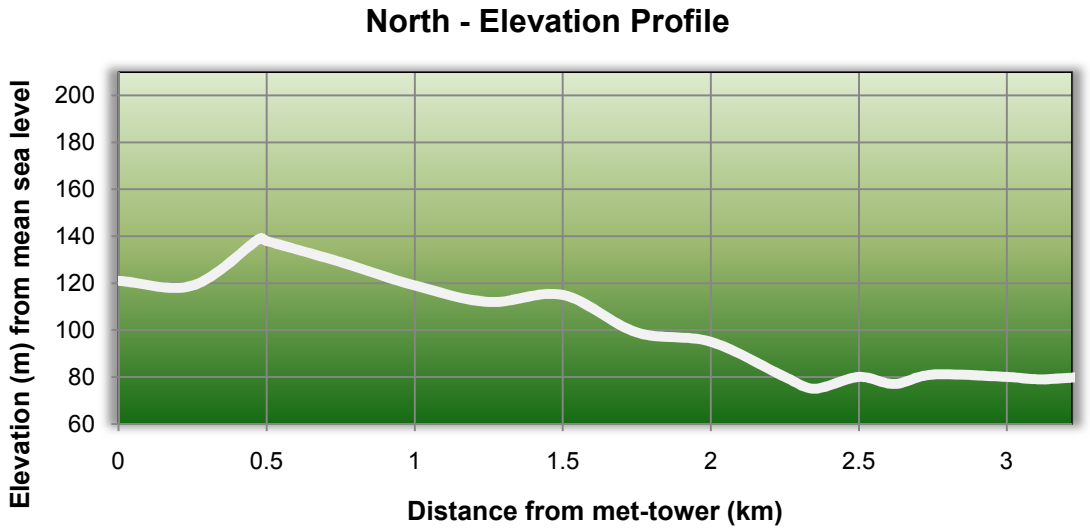

Figure 3-16 : North direction elevation profile for 3.3 km from the Met-tower

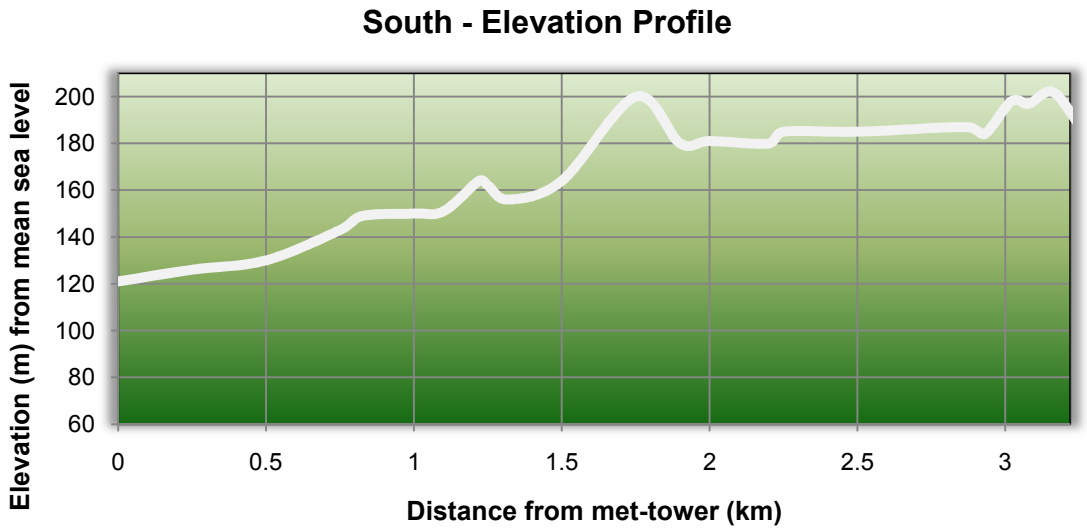

Figure 3-17 : South direction elevation profile for 3.3 km from the Met-tower

A wind rose plot is a useful tool for wind characterization. It is a radial plot that different parameters can be directly presented along there corresponding wind directions around a specific location. For the purpose of the project the area will be distributed in 16 radial zones, each direction corresponds to a 22.5° arc. When referring to a specific direction the data will refer to the values found in a 22.5° range taken the principal direction as the center. For example: North would present 11.25° before and after the true-north (0°). Using *WRPLOT*, a free open source program (Lakes Environmental, 1995), Figures 3-18 to 3-20 were prepared. They present wind rose plots for specific site data for different time periods. Each figure presents the amount of time wind data is collected for a specific direction. The concentric circles represent the percentage of records (time) each direction receives information, having the sum of all directions been 100%. The wind rose plots also presents a distribution of the wind speeds magnitudes for each direction, the color distribution show the presence of individual wind speed ranges as presented in the legend of each wind rose. The “calms” presented as part of the range refer to the wind speed magnitudes below the threshold of 3.0 $m \cdot s^{-1}$ and are not included in the information displayed in the wind rose plots. In addition the wind rose plot show the resulting wind direction vector, the vector accounts for all wind directional data including the “calms” and presents a line that shows the average direction of the wind.

Figure 3-18 presents the wind rose plot for the complete record for the period from April 30, 2011 to April 30, 2012. In Figure 3-18 are shown two predominant wind directions, East and East Southeast where each one account approximately for 27% and 30% of the data. The remaining data is distributed mostly in the East Northeast with almost 14% of the data and the Southeast with about 7%, where the rest is distributed in the remaining directions and represents about 6%. The East and East Northeast direction have wind speed distributions that concentrate in higher magnitudes over 7.0 $m \cdot s^{-1}$, where in the East Southeast and the Southeast directions the magnitudes are lower than 7.0 $m \cdot s^{-1}$. The resulting vector is found to be around 104° from North, meaning that the prevailing wind comes from the interior area of the Island.

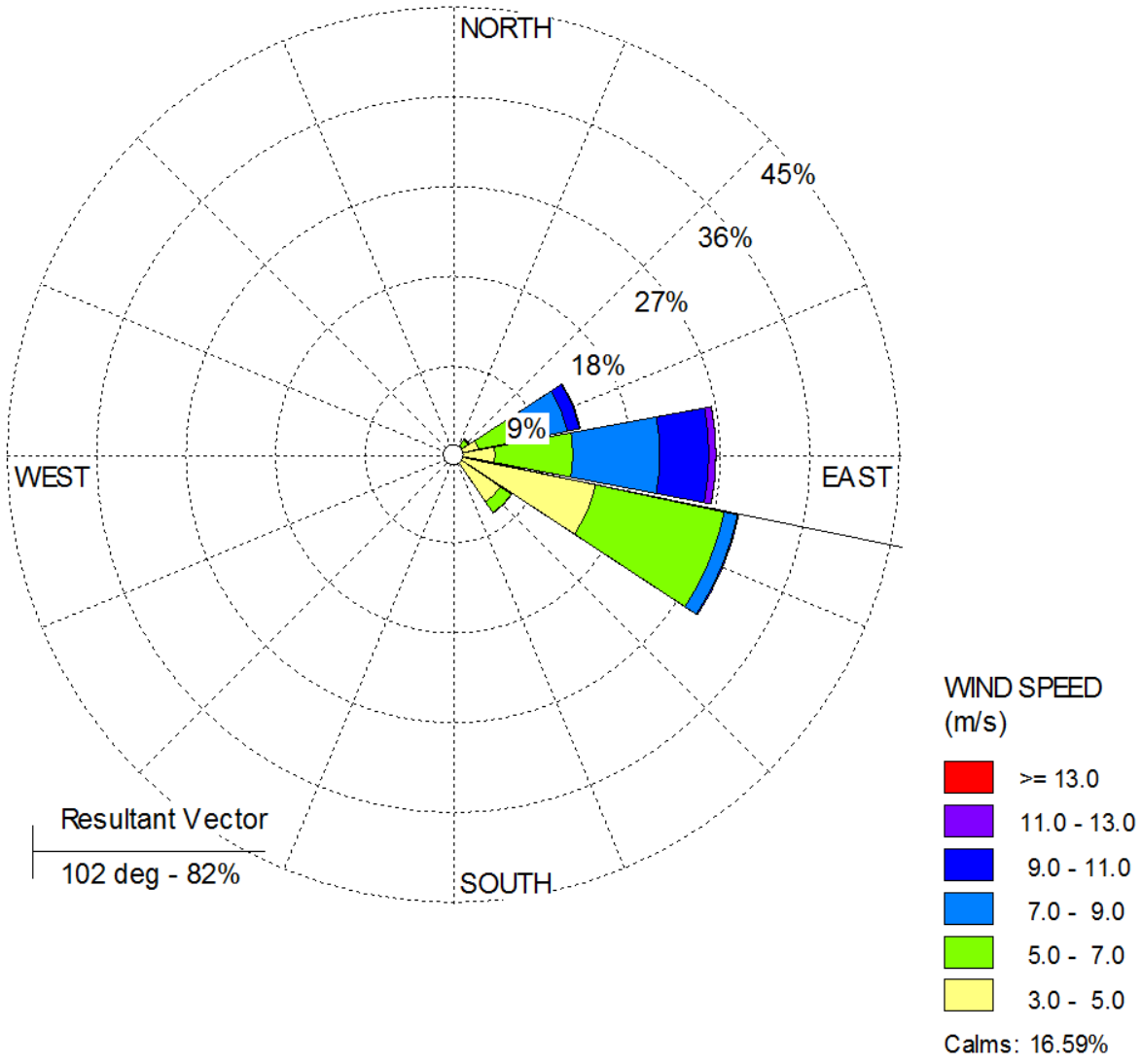

Figure 3-18 : Wind rose plot of all data from Apr-2011 to Apr-2012 for wind speeds at 60 meters (CH02) and wind directions at 58 meters (CH07)

When comparing the wind rose plot behavior for the daytime illustrated in Figure 3-19 and nighttime in Figure 3-20, a clear relationship to Figure 3-18 can be found. The two main wind directions found in Figure 3-18 are separated; the East becomes the predominant wind direction in the daytime and the East Southeast for the nighttime. In the daytime resulting vector moves to 88° where the majority of the wind comes from East Northeast and East directions and have a wind speed distribution favoring the values higher than 7.0 $m \cdot s^{-1}$. This indicates that winds coming from the coastal area in the daytime travel through more uniform terrains. For the

nighttime the resulting vector moves to 114° where the majority of the wind comes from East Southeast and Southeast directions and have a wind speed distribution favoring the values lower than 7.0 $m \cdot s^{-1}$. The change in direction in the nighttime indicates winds that come from the mountain area of the Island that have to travel through terrain with complex topographical features and low rising urban structures.

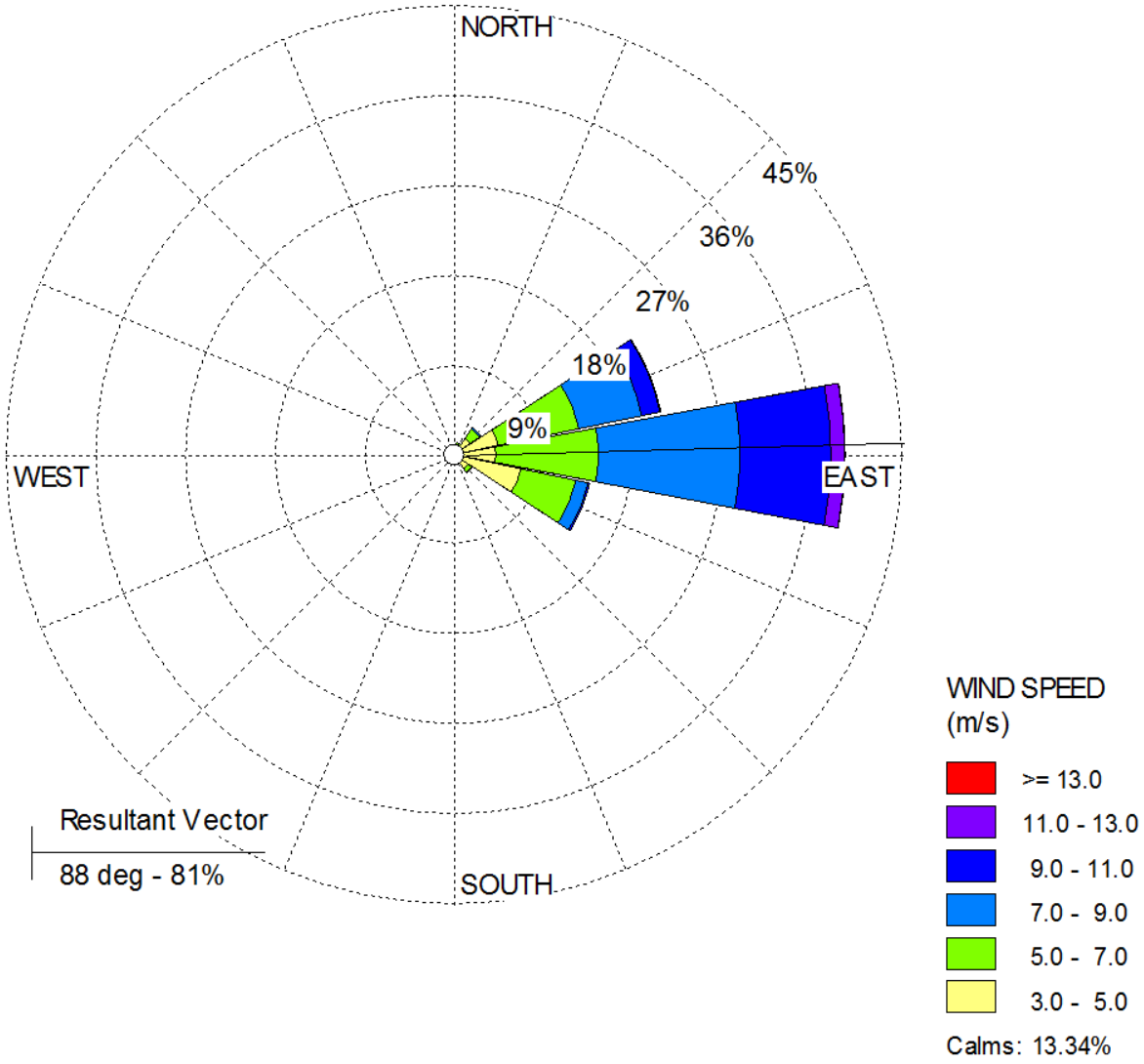

Figure 3-19 : Wind rose plot of daytime data from Apr-2011 to Apr 2012 for wind speeds at 60meters (CH02) and wind directions at 58 meters (CH07)

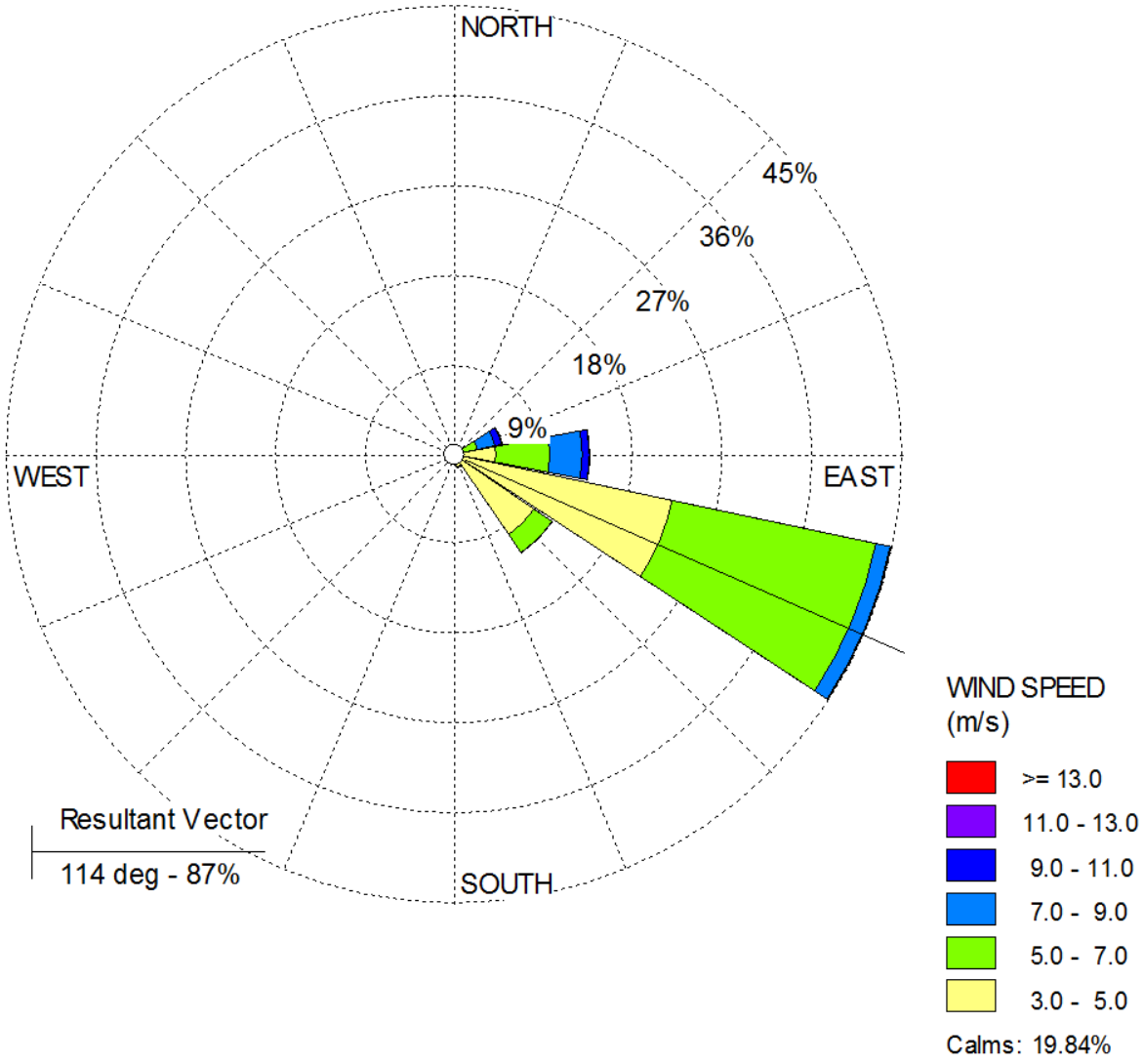

Figure 3-20 : Wind rose plot of nighttime data from Apr-2011 to Apr 2012 for wind speeds at 60 meters (CH02) and wind directions at 58 meters (CH07)

3.3.5 Summary of wind characteristics

Wind characteristics were calculated using the threshold previously presented, over the different time periods and directions. The initial parameters are wind speed and direction, since the latter was only measured at two elevation (fifty eight and thirty eight meters) and correlated well, it is possible to say that both wind vanes, CH07 and CH08, present relatively the same direction. At each elevation two anemometers were located, once each channel was inspected for faulty data and the damage records were remove an average wind speed was determined.

The wind speed average for the purpose of this study was derived arithmetically. Table 3.5 has a summary of the resulting average wind speeds for each elevation and condition presented. As expected the daytime had the highest wind speeds and the nighttime the lowest. The differences in the wind speeds between elevations along the vertical axis were higher in the nighttime presenting a higher variability in the wind's profile, in the daytime the values are closer together.

Table 3-5 : Average wind speed variations

	Wind speed ($m \cdot s^{-1}$)		
Instrument at elevation (m)	**60**	**48**	**40**
Day	5.89	5.61	5.34
Night	4.49	4.02	3.59

One of the most important parameters to characterize the wind's behavior is the power law coefficient, also known as the “wind shear coefficient” (WSC). Even though the WSC has no scientific basis, it can be used to generate an acceptable wind profile and estimated other parameters such as roughness length. The WSC was determined using the alpha equation (Equation 11) for the average wind speeds at each elevation for each sample in each record. Having data for three elevations provides the ability to calculate more than one WSC. In this case three combinations were possible: sixty and forty, sixty and forty eight meters and forty eight and forty meters. The summary of the resulting average WSC and their combined average are presented in Table 3.6. As expected, the coefficients for the day were lower, meaning that the wind profile has less variability between elevations, where as in the night the coefficients are significantly higher. The WSC for the closer elevations have higher values meaning that the profiles are more susceptible to changes in the wind speed velocities.

Alpha equation

$$\alpha = \frac{\ln\left(\frac{u(z)}{u_i}\right)}{\ln\left(\frac{z}{z_i}\right)} \quad (11)$$

Table 3-6 : Wind shear coefficient variations for all available combinations during daytime and nighttime conditions

Elevations	60 m - 40 m	60 m - 48 m	48 m - 40 m	Average
Day	0.24	0.21	0.27	0.24
Night	0.59	0.55	0.63	0.59

The difference in topographical features and exposure conditions around the area of the Met-tower will affect the characteristics of the wind as a function of the direction it traveled. In Table 3-7 it is possible to appreciate the change in the conditions around the area, in the south region the WSC is considerably higher, something that is expected because of the high topographical features and urban area. In the North region, lower coefficients are present due to the predominant uniformity of the terrain, indicative of lower topographic features and a less urbanized sector. The highest coefficients in both the daytime and the nighttime came from the south east direction and the lowest come from the north-west direction. Overall, the coefficients for the night are considerably higher than the ones found in the day.

Table 3-7 : Directional variation of wind characteristics

	Day			Night		
Direction	**Time %**	**Ave. α**	**Ave. wind speed at 60 m ($m \cdot s^{-1}$)**	**Time %**	**Ave. α**	**Ave. wind speed at 60 m ($m \cdot s^{-1}$)**
N	0.69%	0.13	4.00	0.02%	0.37	7.20
NNE	1.57%	0.20	4.00	0.08%	0.44	4.90
NE	3.94%	0.17	4.70	1.00%	0.44	6.20
ENE	24.51%	0.20	6.50	6.30%	0.42	7.00
E	45.28%	0.24	7.60	17.10%	0.45	6.00
ESE	16.17%	0.37	5.10	55.92%	0.62	5.00
SE	2.74%	0.51	4.30	15.05%	0.73	4.30
SSE	1.02%	0.30	4.50	1.91%	0.58	3.90
S	1.17%	0.31	5.10	0.75%	0.55	4.10
SSW	0.97%	0.34	5.60	0.97%	0.51	4.40
SW	0.61%	0.34	6.20	0.64%	0.58	5.20
WSW	0.33%	0.23	6.70	0.20%	0.46	4.20
W	0.17%	0.16	6.70	0.03%	0.32	4.20
WNW	0.24%	0.09	5.60	0.01%	0.23	6.90
NW	0.07%	0.06	4.40	0.00%	0.19	9.20
NNW	0.52%	0.19	4.10	0.01%	0.33	9.40
Σ	100%			100%		

Turbulence intensity (TI) as defined in Equation 4 was calculated for the different conditions and the results are presented in Table 3-8. The average turbulence intensity for each sample was calculated using the standard deviation (SD) and average wind speed of the present in each data point recorded in the channels. The resulting values in Table 3-8 are the average of the all values in the record. When comparing the results the turbulence intensity decreases for all cases when the elevation increases, this is expected since the variability in wind is expected to decreases as the elevation increases. The behavior of the TI is different than expected when comparing nighttime and daytime, where smaller values are found in the nighttime. These could be due to the behavior of the wind in the ten minute sample time, referring to a higher variability in the sample time for the daytime.

Table 3-8 : Average turbulence intensity for each sample by elevation and condition

	Average Turbulence intensity (TI) for data samples		
Elevations	**60 m**	**48 m**	**40 m**
Day	15%	17%	18%
Night	11%	13%	15%

The final parameter evaluated is the energy potential for the area; it is depicted in the wind rose plot in Figure 3-23 using Belt's limit equation (Equation 6) and an air density of 1.16 kg/m^3. The air density was determined in relation to typical air temperature of twenty five degrees Celsius. In this case the energy total produce in both daytime and nighttime is sum together and divided by the individual production of each direction. The new percentage can be used to better determine the energy conditions of the site without selecting a specific turbine for sweep area. The energy potential is almost completely in the daytime, this is expected due to higher wind speeds. The energy would almost completely come from the east, meaning that the WSC for this direction would have the greater impact in energy production.

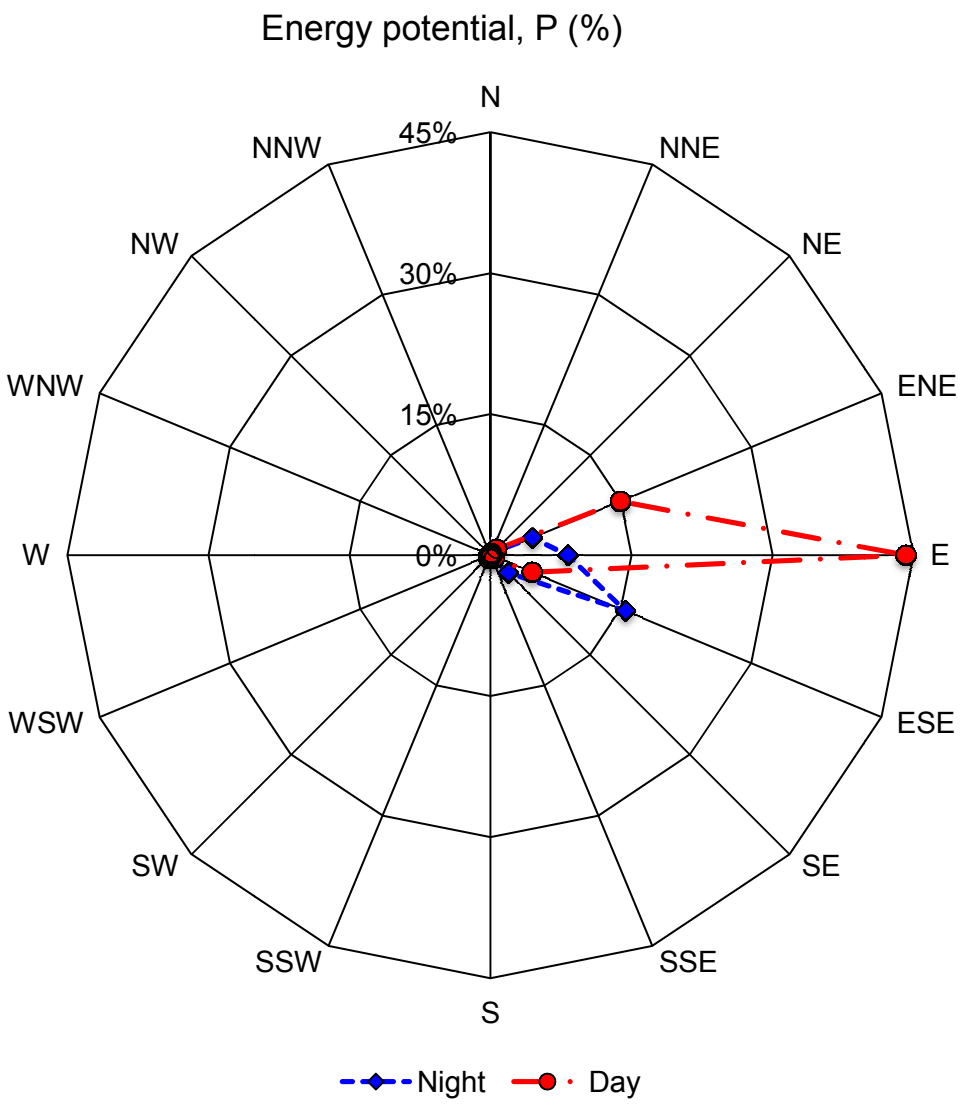

Figure 3-21 : Energy potential for the Isabela Met-Tower site @ 60 meter by direction, PR

CHAPTER 4. **Wind profiles assessment**

In order to simulate site conditions and tower parameters, it is necessary to create a model that adequately represents them. The first step requires gathering all necessary available data for the site in question: location, in situ wind data, and adjacent features that may affect wind flow. The available site information and wind characteristics allow for the assessment of wind profiles models for different site conditions like the diurnal, nocturnal and directional variations.

4.1 Wind mean speed vertical profiles (Wind Profiles)

The in-situ wind data are used to generate wind-profiles models that correspond to site conditions. A vertical wind profile represents the change in mean wind speed as a function of height. In this report, vertical wind profiles use the power law model. Figure 4-1 shows the variation in the vertical wind profile when the reference mean wind-speed varies plus and minus two standard deviations. This fluctuation represents 95% of the mean wind-speed $\bar{U}$. Variations in the mean speed wind profile have significant effects in wind turbine efficiency and the loads acting in wind turbine components like the tower and rotor blades. Such variations can be present in extreme wind conditions; however, it is the cumulative fatigue effects over time that can be easily overlook.

Table 4.1 presents the wind speed range for diurnal and nocturnal cycles that can reasonably be expected within 95% confidence interval of a normal distribution of the mean wind-speed $\bar{U}$ at 60 meters and their average wind shear coefficient (α). The range presented stands for a variation of two standard deviations (σ), plus and minus, from the mean value. The values for the average wind shear coefficient were calculated as defined in the previous chapter. As expected the diurnal average wind shear is lower than the nocturnal one by less than a half. However, the diurnal value of the mean wind-speed is higher.

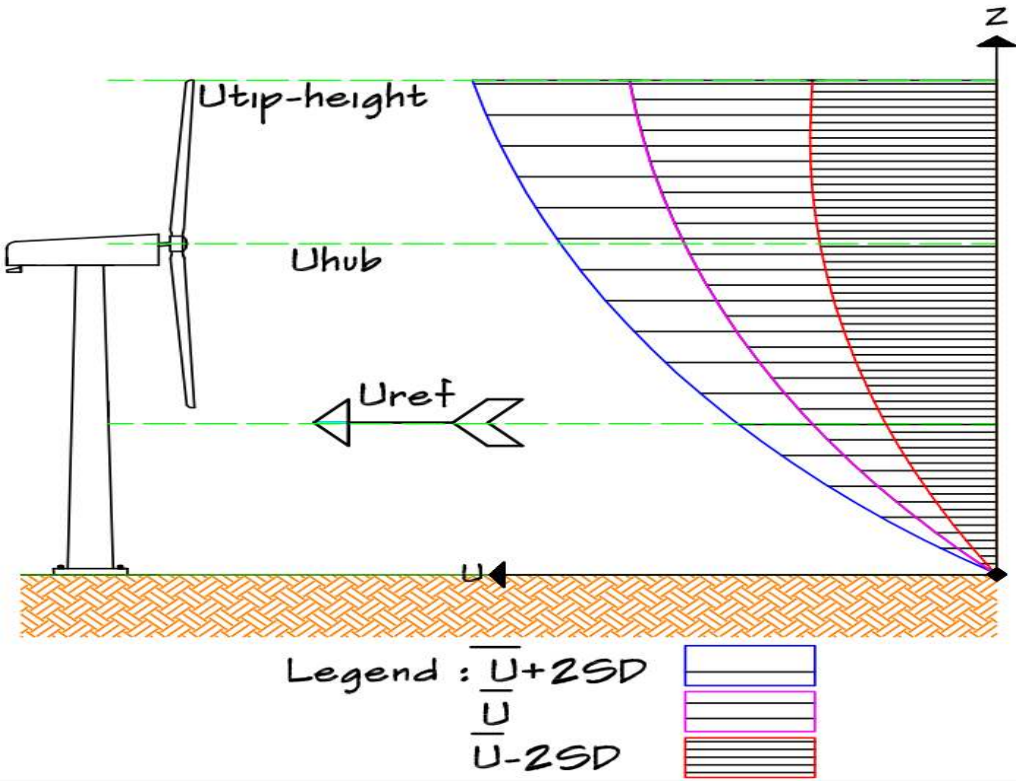

Figure 4-1: Representation of vertical wind speed profile variation.

The change in wind shear and wind speed can be better appreciated when they are related to their primary wind directions as displayed earlier in Chapter 3 in Figures 3-17 and 3-18 for the diurnal and nocturnal cycles, respectively. It was found that the nocturnal wind direction approaches from complex mountain terrain in the East to South region; this will increase the mechanical turbulence and leads to higher wind shear. In the daytime, wind comes from the coastal zone (North to East region) and travels through a more uniform terrain with less topographic features but higher wind speed from the ocean and coast thermal interaction.

Table 4-1 : Diurnal and nocturnal wind characterization variations

	Mean α	$\bar{U}$ 60m $m \cdot s^{-1}$	σ $m \cdot s^{-1}$	$\bar{U} - 2 \cdot \sigma$ $m \cdot s^{-1}$	$\bar{U} + 2 \cdot \sigma$ $m \cdot s^{-1}$
Diurnal cycle	0.26	5.89	2.12	1.65	10.13
Nocturnal cycle	0.59	4.49	1.43	1.62	7.36

The wind profile variation in the vertical axis depends on two variables (1) the reference wind-speed and (2) the wind shear coefficient, as defined in Equation 2. Figure 4-2 to 4-3 shows

the variation in the wind profile for the diurnal and nocturnal cycles respectively, for the upper, mean and lower values of the reference wind speed presented in Table 4-1. The vertical variation for these figures is set to begin at 10 meters up to 150 meters. This will accommodate a relatively high tip-height which is the hub height plus the radius of the rotor. The wind profiles representing the mean, upper and lower confidence limits at sixty meters are identified with square, triangular and circular markers, respectively. For both conditions cycle conditions the lower confidence interval limit reveals wind-profiles with the least pronounce curvatures this indicates that the changes in wind-speed would be small in the vertical axis. The wind profile of the mean and upper confidence interval have a higher curvature, meaning that the changes in wind speed are more pronounced than the lower boundary, specially the upper boundary. Comparing both figures it is essential to note that in the nocturnal cycle, the wind speeds are lower than the diurnal up to the reference height of 60 m. For vertical elevations above the reference speed height, the wind speeds in the two daily cycles become and even the nighttime velocity can overtake the daytime one for the lower confidence limit and the mean speed. This pattern (the nighttime speed overtaking the daytime) also occurs for the upper confidence limit for vertical elevations above the tip height of 150 meters. This behavior of the wind profile can be attributed to the higher wind shear coefficient observed in the nighttime.

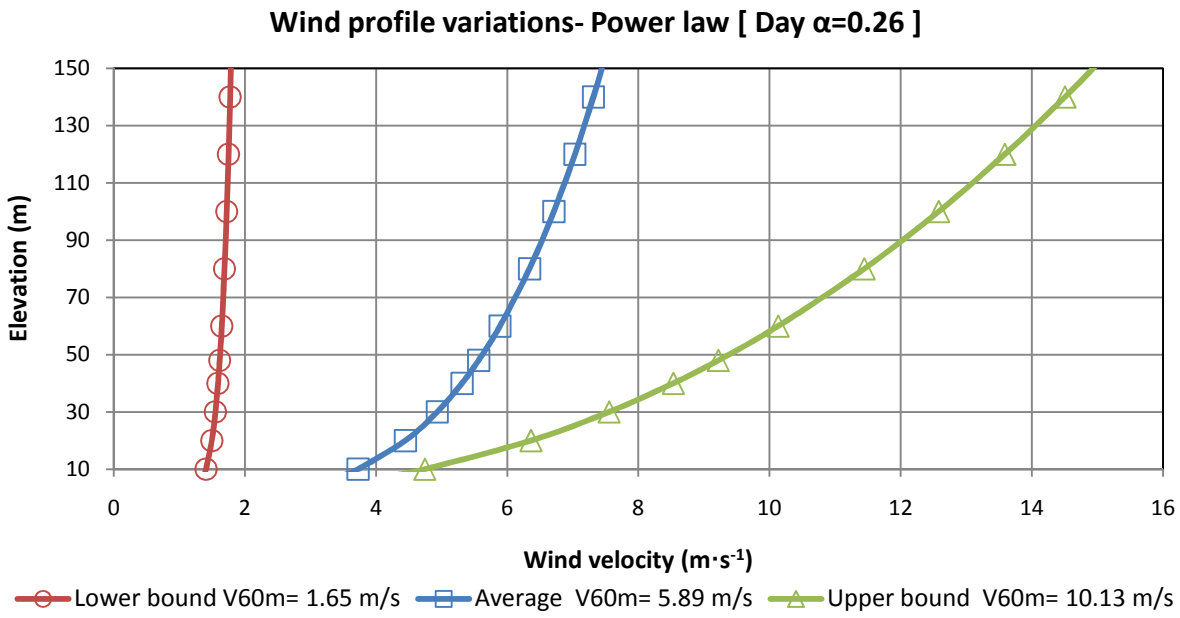

Figure 4-2 : Wind profile variation during daytime

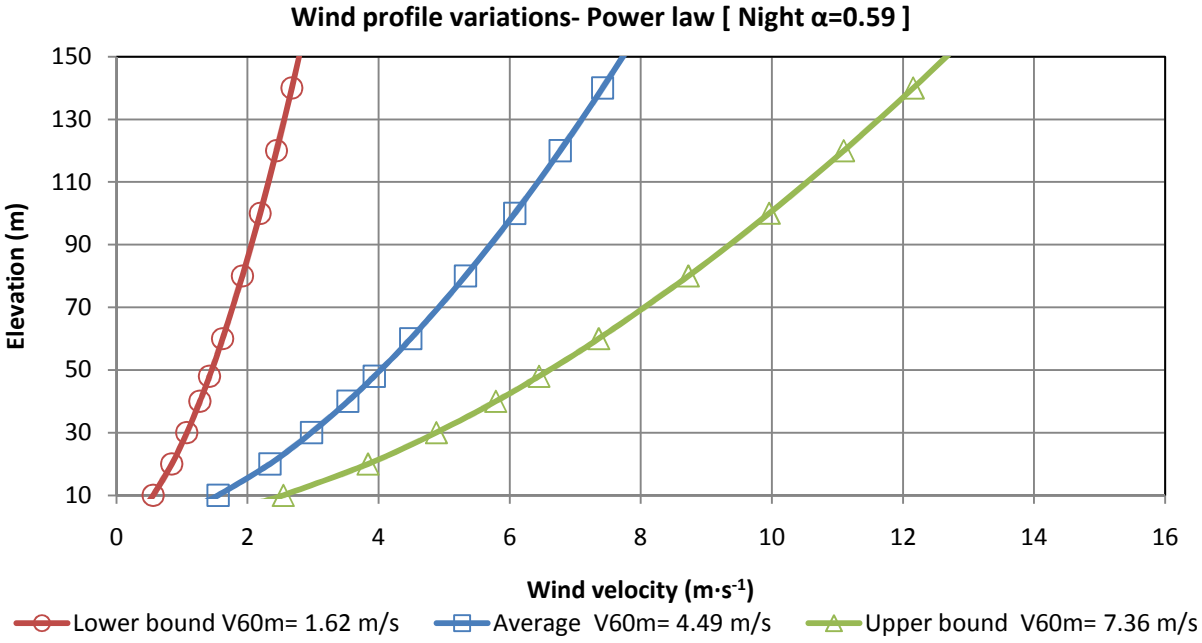

Figure 4-3 : Wind profile variation during nighttime

As presented previously in Chapter 3, the direction along which the wind travels can have a considerable effect on its behavior. Using the average wind speed at 60 meters and its corresponding wind shear coefficient it is possible to create wind profiles for each direction; the results were presented in Table 3-7. In Figures 4-4 and 4-5, the individual profiles are presented by quadrants for both day and night conditions. Each quadrant represents a 90° arc segment around the Met-tower divided. The circle among the tower is divided as follows: first-quadrant from North to East, second-quadrant from East to South, third-quadrant from South to West and fourth-quadrant from West to North. The quadrants are further subdivided, into four directions, each with a 22.5 degrees angle, beginning in the North at 348.75° (or -11.25°) to 11.25° degrees and progressing until a 360° rotation is completed.

The nighttime profiles use high overall WSC (higher then 0.3) and produce wind speed changes more rapidly as the elevation changes. The profiles of the first two quadrants of the nighttime are similar in magnitude and behavior both begin at 10 m around 2 m*s-1 and reach velocities between 6 and 10 m*s-1. The first two quadrants of the nighttime have the dominant wind directions. The wind speed magnitude of the profiles in the third quadrant decrease when compared to the previous two but they maintain their high WSCs. In the fourth quadrant, the profiles are less uniform and have more variability between directions. The variability in the profiles of the fourth quadrant is most likely because of the low frequency of wind coming from these directions. The diurnal cycle over-all has lower WSC then the nocturnal cycle that produce profiles more uniform and have with less variability by elevation. In the first two quadrants of the daytime, the profiles belonging to the E and ENE have the highest wind speeds magnitudes for the cycle and correspond to dominant wind directions of the daytime. The East profile of the daytime has the highest magnitude profiles of both day and night only overtaken by the nighttime profiles of the North and ENE for the elevations higher than 60 m. Similar to the nocturnal cycle the third quadrant of the diurnal cycle has lower magnitude profiles. The fourth quadrant has more variability in its directional profiles due to the lower frequency in the wind that comes from that direction.

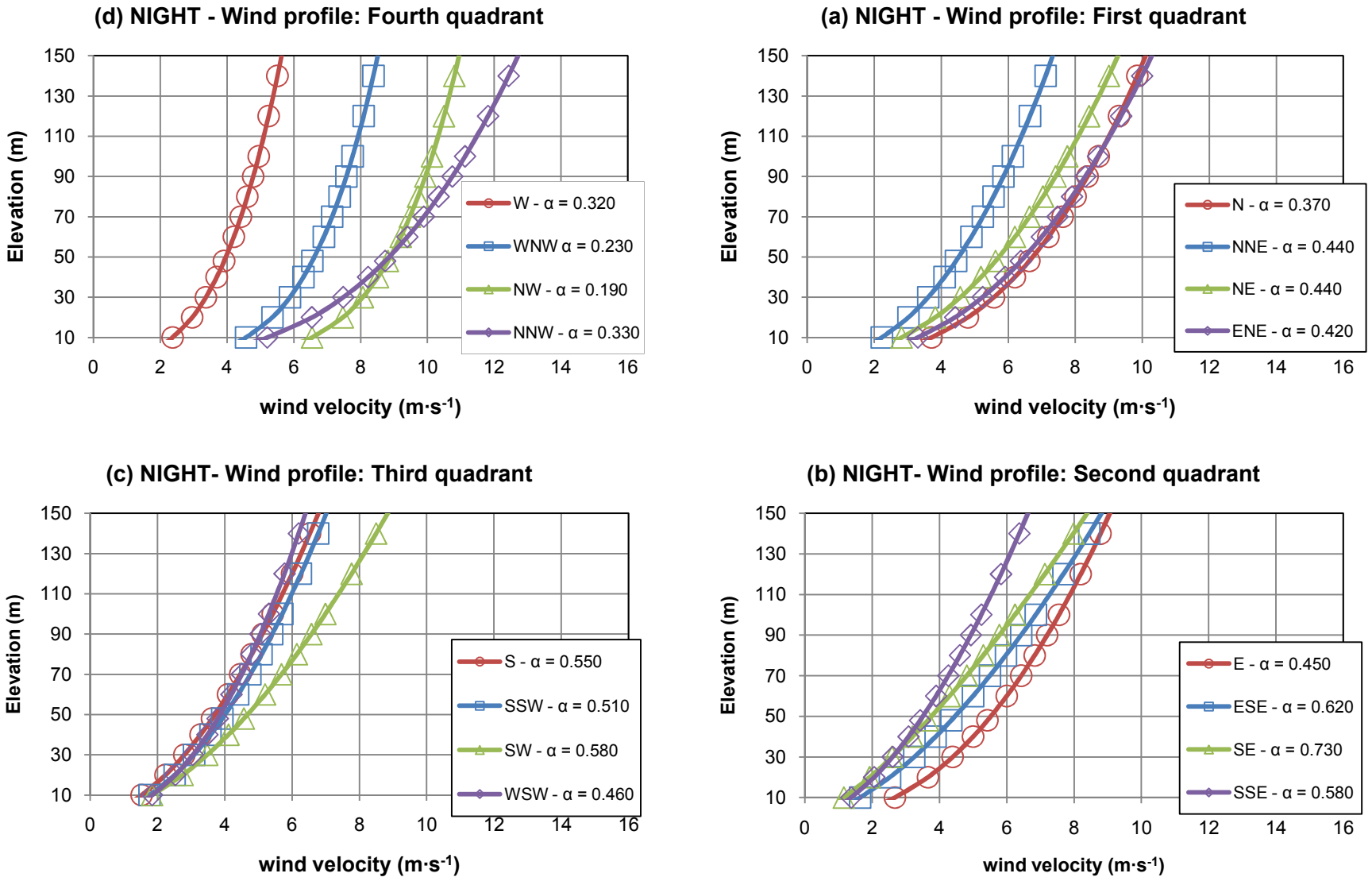

Figure 4-4 : Nighttime wind profiles by direction:

a) First quadrant, b) Second quadrant, c) Third quadrant, and d) Fourth quadrant

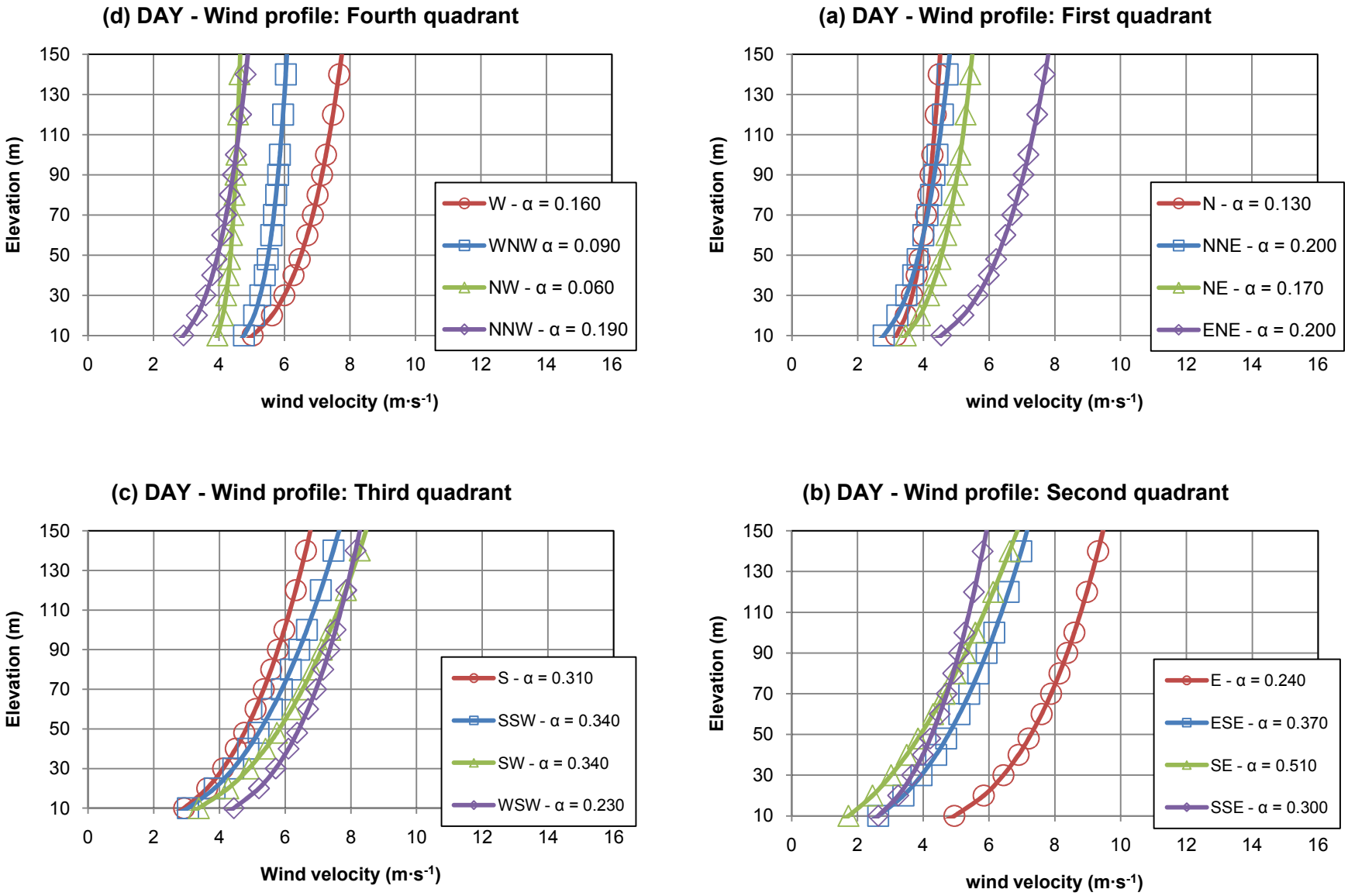

Figure 4-5 : Daytime wind profiles by direction:

a) First quadrant, b) Second quadrant, c) Third quadrant, and d) Fourth quadrant

Figures 4-6 and 4-7 have a selection of the two quadrants that have the overall higher and lower wind speeds magnitudes for the wind-profiles. These figures incorporate the three directions that presented the lower and higher boundaries of the wind speed creating a range that incorporates the possible wind speeds for each selected quadrant. The first quadrant for both day and night has the lower magnitude profiles, however, in the nighttime the wind shear in these directions are considerably higher than the daytime but have the lower reference wind-speeds. The fourth quadrant in the nighttime has the highest magnitude wind speeds in the NNW and the NW, but they account for an extremely small percent of time for the entire record, less than 0.02% of the nighttime. At daytime, the second quadrant has the higher magnitude profiles, having the highest magnitude the wind-profile when the wind travels from the East direction representing 45 % of the daytime measurements.

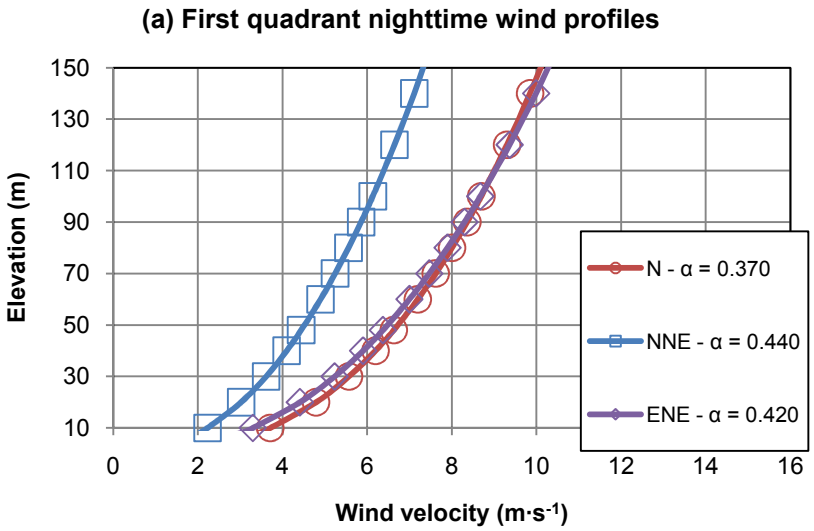

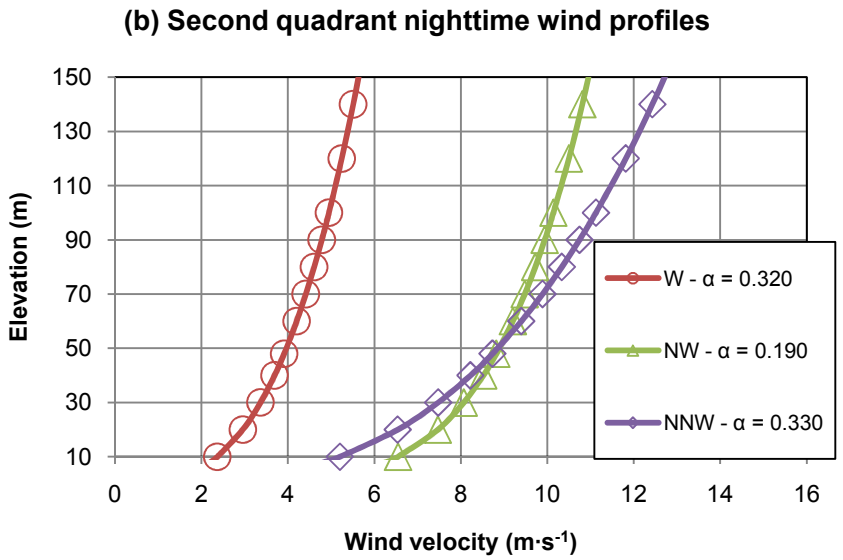

Figure 4-6 : Nighttime wind profiles by direction: a) First quadrant and b) Fourth quadrant

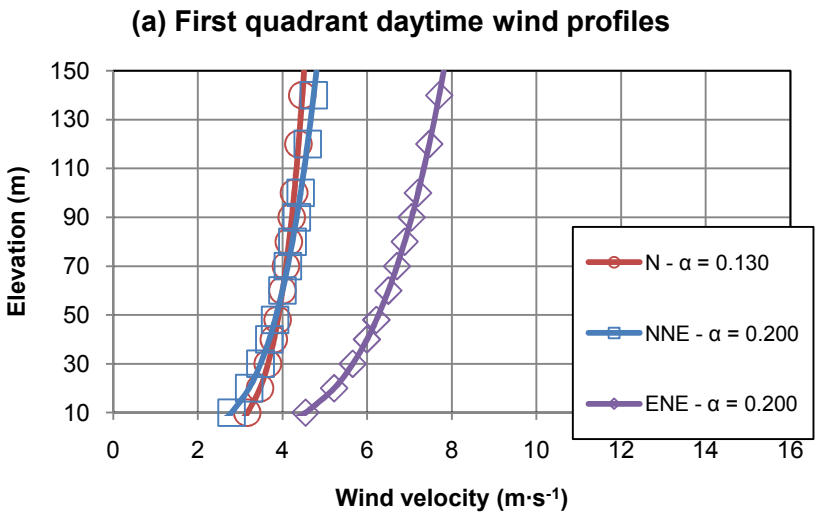

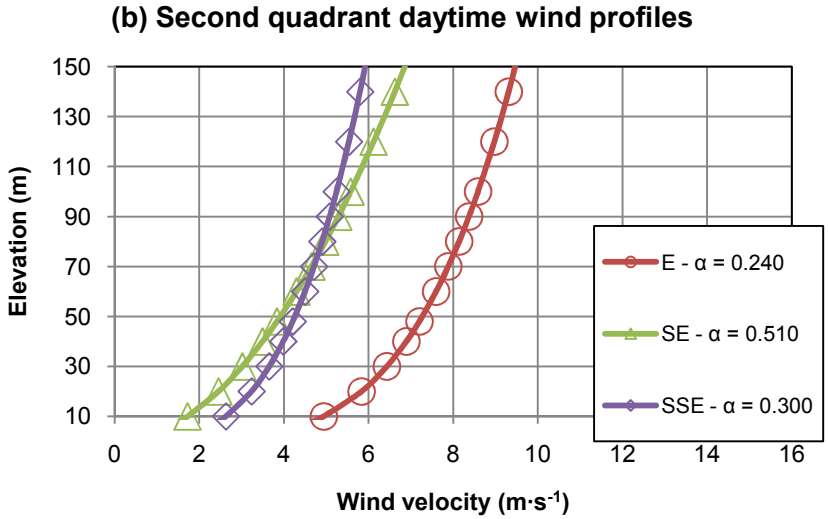

Figure 4-7 : Daytime wind profiles by direction: a) First quadrant and b) Second quadrant

CHAPTER 5. **Conclusions and Recommendations**

5.1 Conclusions

The wind characteristics of the Isabela Met-Tower site indicate that this location is promising for the use of wind energy generators. The intensity of the wind speed at the highest elevation of the Met-tower, 60 meters, indicates viable wind energy resource for energy generation. The diurnal wind cycle indicates that it would yield the most energ, since it has the highest wind speeds and the more uniform distribution of high wind speed magnitudes. In the nocturnal cycle wind conditions change significantly, the wind velocity becomes more localized around magnitudes close to the cut-in velocities, yielding less potential for energy generation. Because the energy consumption tends to be higher in the daytime and the wind's speed intensity is also higher in this time, the energy potential and consumption correspond closely to one another.

Wind shear coefficients (WSC), α, are considerably higher when compared to the IEC (International Electrotechnical Commission (2005)) considerations for wind turbine classes 1 to 3, of around 0.2. High wind shear coefficients (WSC) would potentially yield higher energy production when using higher hub heights, but could have the opposite effect for lower hub heights. The high WSC can produce eccentricities in the wind loading of the structure since the loading is not uniform and will vary considerably along the vertical length of the tower. This would increase the likelihood of fatigue damage especially in the blade assembly. The northern farmland region of the Isabela site presents higher wind speeds and lower WSC, where as the southern region has lower wind speeds and higher WSC.

The wind primarily comes from the east: during daytime the wind direction shifts to the North-East quadrant coming from the shore and in the nighttime it shifts to the South-East quadrant coming from the mountain region. To analyze further the behavior of the wind as it

travels through the surrounding area a Weather Research Forecast (WRF) model could be use. WRF is a three dimensional wind model for the prediction of wind speeds and direction utilizing topography data and large scale meteorological data inputs.

NREL's design codes prove to be a resourceful and accessible tool as presented in Appendix A. The main difficulties with the use of the program are keeping track of the changes and modifications for each “run”, given the number of input text files it uses. To analyze the conditions in the Met-tower area, several key components for modeling need to be addressed, since the turbine that would be appropriate for the conditions of the Isabela Met-tower is an “S-Class”. Little information or guidelines are currently available for this class since the IEC standards does not go into details as it does for the other turbine class. The specifications of the “S-class” turbines need to be provided by the turbine manufacturer. In addition, the WSC for the region are higher than the values standard values for wind turbines classifications I, II and III, that have WSC no higher than 0.2 (International Electrotechnical Commission, 2005). These two conditions are additional factors to consider in any load calculation for any turbine alternative for this location. The turbine selection must then consider: monthly mean horizontal wind speeds from 4 $m \cdot s^{-1}$ to 6.2 $m \cdot s^{-1}$ at 60 meters, higher WSC conditions that include values up to 0.7 and hurricane wind speeds. The hurricane wind speeds must account for the roughness conditions in the area, at least a 50 year recurrence period and the sudden changes in the direction of the wind possibly, a modified ECD of the IEC.

The implications of an S-class turbine should also include the study of the special conditions of the class. It is important to note that the high WSC (α) may not constitute an initial problem, but it could lead to more wear and tear on the structure and it could reduce the life expectancy and increase maintenance costs. It is likely that for most locations around the Island, future wind energy developments will require “S-class” turbines and many sites might share similar roughness variations leading to high WSC. The understanding of these factors will play a critical role in any successful long-term development of wind energy in the Island.

5.2 **Recommendations**

In order to better understand yearly variability of the data analysis presented on this report it may be feasible to incorporate the entire data record, which now consists of more than 2 years of data (April 2011 to May 2013). Numerical weather prediction (NWP) models can be employed and validated with the Met-tower data such as the Weather Research and Forecasting (WRF) Model currently implemented as part of the Caribean Coastal Ocean Observation System (2013) or CariCOOS for its initials. The model could be used to study the roughness features (topography, vegetation and structures) and thermal variation (day and night time). A calibrated NWP model will serve as an assessment tool for other prospective site along Puerto Rico. Upgrade the wind anemometers in order to collect 3D components of the wind (along, across and vertical) at higher sampling rates (1Hz), and include telemetry capability to gather the data remotely to automate the data analysis on daily basis. Finally to to assess the feasibility of an wind energy installation the following parameters should be study: the turbine class (S-class) characteristic should comply with site conditions, cost analysis for a chosen turbine, and further studies on environmental impact.

References :

AIJ-RLB-1996, 1996. Recommendations for Loads on Buildings. Architecture Institute of Japan (English version. 1996)

Altaii, K., & Farrugia, R. (2003). Wind characteristics on the Caribbean island of Puerto Rico. *Renewable Energy* , (28) 1701-1710.

American Society of Civil Engineers, ASCE 7-05, Minimum Design Loads for Buildings and Other Structures, Reston, VA, 2005.

Buhl Jr., M. L., & Manjock, A. (2006). A Comparison of Wind Turbine Aeroelastic Codes Used for Certification. *44th AIAA Aerospace Sciences Meeting and Exhibit* Nevada, Reno: National Renewable Energy Laboratory, pp. 1-17.

Caribbean Coastal Ocean Observation Systems. (n.d.). *WRF 2Km NWS-CariCOOS Mirror Run*. Retrieved February 27, 2013, from caricoos.org: http://www.caricoos.org/drupal/es/node/215

Google Earth. (February 16, 2009). *Isabela, Puerto Rico*. Retrieved March 05, 2012, from latitud 18.469467 deg, longitud -67.048407 deg : http://www.google.com/earth/index.html

Holmes, J. D. (2001). *Wind Loading of Structures.* 29 Spon Press, New York.

International Electrotechnical Commission, IEC (2005). *Wind turbines IEC 61400-1.* Geneva, Switzerland.

Lakes Environmental . (1995). *Lakes Environmental Software*. Retrieved March 21, 2012, from http://www.weblakes.com/products/wrplot/index.html

Li, Q., & Zhi, L. (2010). Boundary layer wind structures from observations on 325 m tower. *Journal of Wind Engineering and Industrial Aerodynamics* , (98) 818-832.

Lo Brano, V., Orioli, A., Ciulla, G., & Culotta, S. (2001). Quality of wind speed fitting distributions for the urban area of Palermo, Italy. *Renewable Energy* , 1026–1039.

Masters, F. J. (2004). Measurement, modeling and simulation of ground-level tropycal cyclone winds. University of Florida, Gainesville, Florida, USA.

Morell, J., Corredor, J., Canals, M., Detrés, Y., Aponte, L., Mercado, A., et al. (2012). *Education-CariCOOS.org.* Retrieved March 14, 2013, from The Caribbean Coastal Ocean Observing System-CariCOOS.org: http://storage.caricoos.org/education/modulo/climas_costeros.pdf

NRG Systems, Inc. *NRG Systems.* Retrieved April 4, 2012, from http://www.nrgsystems.com/TechSupport/SoftwareDownloads.aspx

NWTC Computer-Aided Engineering Tools (AeroDyn by David J. Laino, Ph.D.). http://wind.nrel.gov/designcodes/simulators/aerodyn/. Last modified February 23, 2013; accessed March 01, 2013.

NWTC Computer-Aided Engineering Tools (FAST by Jason Jonkman, Ph.D.). http://wind.nrel.gov/designcodes/simulators/fast/. Last modified February 27, 2013; accessed March 01, 2013.

NWTC Design Codes (WindMaker by Dr. David J. Laino). http://wind.nrel.gov/designcodes/preprocessors/windmaker/. Last modified May 06, 2005; accessed March 01, 2013.

Rohatgi, J. S., & Nelson, V. (1994). *Wind Characteristics: an Analisis for Generation of Wind Power.* Alternative Energy Institute, Canyon, Texas.

Schott, T., Landsea, C., Hafele, G., Lorens, J., Taylor, A., Thurm, H., et al. (August 31, 2013). *National Weather Service r.* Retrieved 3 14, 2013, from National Hurricane Center: http://www.nhc.noaa.gov/aboutsshws.php

Second Wind Company, *Second Wind Systems Inc* ,Retrieved June 7, 2012, from http://www.secondwind.com/About

Securing American Energy | *The White House*. (2011, March 30). Retrieved February 10, 2012, from The White House: http://www.whitehouse.gov/energy/securing-american-energy#energy-menu

Singht, S., Bhatti, T. S., & Kothari, D. P. (2006). A review of Wind-Resource-Assesment Technology. *Journal of Energy Engineering*, 8-14.

Solari, G. (2007). The International Association for Wind Engineering (IAWE): Progress and prospects. *Journal of Wind Engineering* , (95) 813–842.

U.S. Department of Energy Renewable Energy Laboratory, Puerto Rico and U.S. Virgin Islands - 50 m Wind Power. (June 19, 2007) Retrieved February 11, 2012. Retrieved from http://www.nrel.gov/gis/images/eere_wind/pr_vi_wind.jpg

U.S. Energy Information and Administration. (2012). *U.S. Energy Information Administration (EIA)*. Retrieved February 10, 2012, from Puerto Rico - U.S. Energy Information Administration (EIA): http://205.254.135.7/state/territory-energy-profiles.cfm?sid=RQ

Appendix A: NREL Design Codes

The International Electrotechnical Commission (IEC) provides standards, regulations and minimum design requirements for the development of wind turbines. The required conditions for structural loads are presented in section 7 titled “Structural design” (International Electrotechnical Commission, 2005). The design loads consider normal operating conditions and extreme wind conditions, as presented in Table 2 section 7.4 of the IEC standards (International Electrotechnical Commission, 2005), as indicated in Table A-1. The IEC standards incorporate various design load cases to account for the ultimate loads as well as fatigue loads. The NREL codes use the IEC standards to determine the loads that a wind turbine will experience during different events depending on an established wind condition. In Figure A-1 it is illustrated a diagram that depicts the basic idea for the procedure of simulating the load conditions for a wind turbine with NREL's codes. The initial information required is the wind site characteristics and structural parameters of a proposed wind turbine. With the first information it is possible to estimate the site wind power and also proceed to calculate the IEC wind conditions. These conditions can be modeled using the *Windmaker* or *IECWind* codes from NREL. Once the wind conditions have been established and using additional structural information of a proposed wind tower (i.e., mass, dimensions, tower parameters, nacelle and blades), it is possible to run *AeroDyn* and *FAST*® (simultaneously). The results of the analysis obtained from *FAST*® provide time series outputs that can be used to check the capacity of the structural components and design the tower foundation.

Table A-1 : IEC Design load cases as define in the its third edition

Design Situation	Design Load Case	Wind Condition	Analysis Class	Partial safety factor	Design Situation
1) Power production	1.1	NTM $V_{in} < V_{hub} < V_{out}$	For extrapolation of extreme events	U	N
	1.2	NTM $V_{in} < V_{hub} < V_{out}$		F	*
	1.3	ETM $V_{in} < V_{hub} < V_{out}$		U	N
	1.4	ECD $V_{hub} = V_r - 2m \cdot s^{-1}, V_r, V_r + 2m \cdot s^{-1}$		U	N
	1.5	EWS $V_{in} < V_{hub} < V_{out}$		U	N
2) Power production plus occurrence of fault	2.1	NTM $V_{in} < V_{hub} < V_{out}$	Control system fault or loss of electrical network	U	N
	2.2	NTM $V_{in} < V_{hub} < V_{out}$	Control system or preceding internal electrical fault	U	A
	2.3	EOG $V_{hub}=V_r \pm 2\ m \cdot s^{-1}$, and V_{out}	External or internal electrical fault including loss of electrical network	U	A
	2.4	NTM $V_{in} < V_{hub} < V_{out}$	Control, protection, or electrical system faults including loss of electrical network	F	*
3) Start up	3.1	NWP $V_{in} < V_{hub} < V_{out}$		F	*
	3.2	EOG $V_{hub} = V_{in}, V_r \pm 2\ m \cdot s^{-1}$, and V_{out}		U	N
	3.3	EDC $V_{hub} = V_{in}, V_r \pm 2m \cdot s^{-1}$, and V_{out}		U	N
4) Normal shut down	4.1	NWP $V_{in} < V_{hub} < V_{out}$		F	*
	4.2	EOG $V_{hub} = V_{in}, V_r \pm 2m \cdot s^{-1}$, and V_{out}		U	N

Design Situation	Design Load Case	Wind Condition	Analysis Class	Partial safety factor	Design Situation
5) Emergency shut down	5.1	NTM $V_{hub} = V_{in}$, $V_r \pm 2m \cdot s^{-1}$, and V_{out}		U	N
6) Parked (standing still or idling)	6.1	EWM 50-yr recurrence period		U	N
	6.2	EWM 50-yr recurrence period	Loss of electrical network connection	U	A
	6.3	EWM 1-yr recurrence period	Extreme yaw misalignment	U	N
	6.4	NTM $V_{hub} < .7 * V_{ref}$		F	*
7) Parked and fault conditions	7.1	EWM 1-yr recurrence period		U	A
8) Transport, assembly, maintenance and repair	8.1	NTM V_{main} to be stated by the manufacturer		U	T
	8.2	EWM 1-yr recurrence period		U	A

where :

NTM - Normal wind profile model,
ETM - Extreme turbulence model,
ECD - Extreme coherent gust with direction change,
EWS - Extreme wind shear,
EOG - Extreme operational gust,
NWP - Normal turbulence model,
EDC - Extreme direction change,
EWM - Extreme wind speed model,
V_{hub} - Hub height wind speed,
V_{ref} - Wind speed at reference height,
V_r - Rated Wind speed,
$V_r \pm 2m \cdot s^{-1}$ - Sensitivity to all wind speeds in the range shall be analysed,
V_{in} - Extreme coherent gust with direction change,
V_{out} - Extreme coherent gust with direction change,
F - Fatigue,
U - Ultimate strength,
N - Normal,
A - Abnormal,
T - Transport and erection, and
* - Partial safety for fatigue.

In the case of Puerto Rico the IEC standards classifies the wind conditions as S-class, this means that the normal design conditions have to account for hurricane conditions. The responsibility for accounting for the "S-class" condition falls under the wind turbine manufacturer.

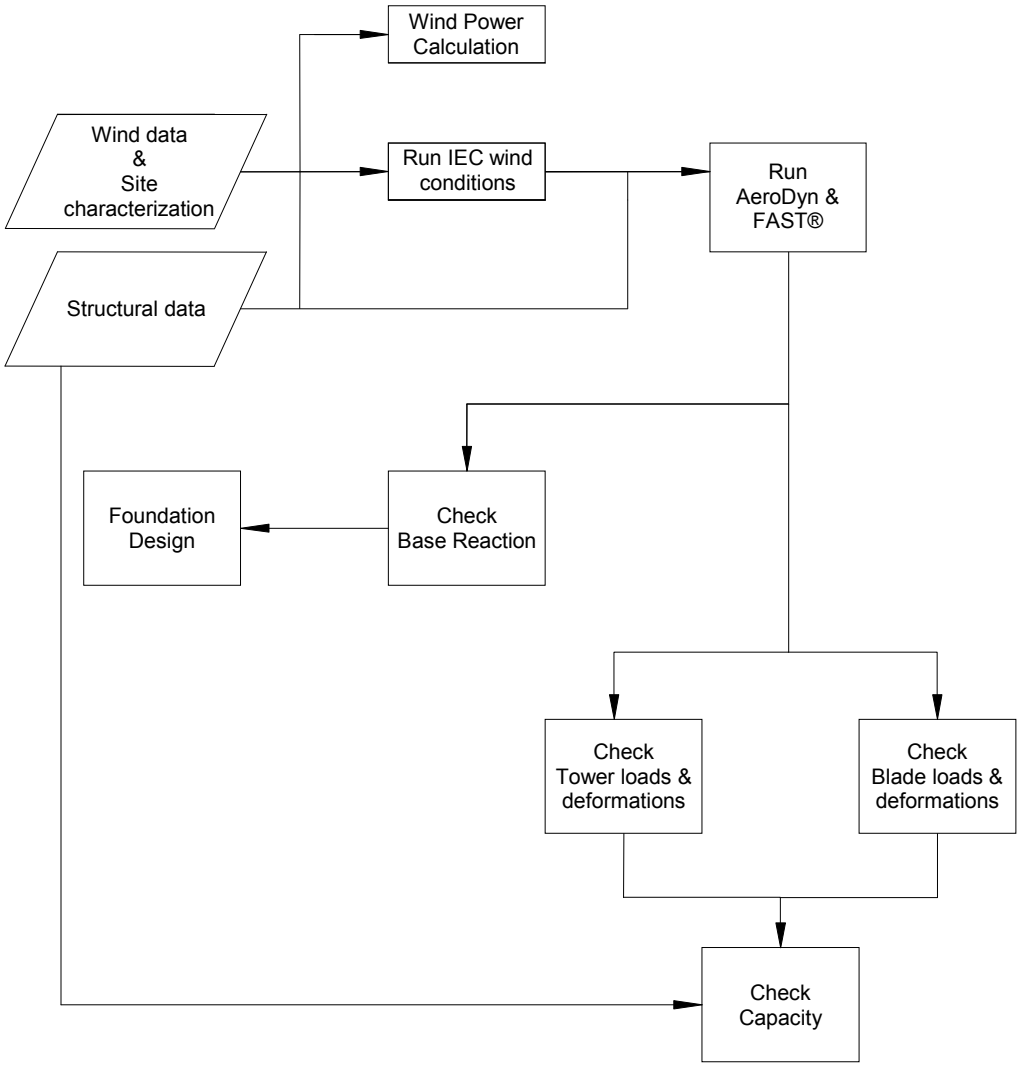

Figure A-1 : Flowchart for wind turbine load assessment using NREL codes

A.1 Example of NREL code run - Certification test 12

The structural properties of any commercial turbine are strictly protected by each manufacturer. The specifications can be used to determine a variety of parameters related to power production and efficiency. For the purpose of this project, because of the restriction in information on S-class turbines, an example of *FAST*® is used to describe the capabilities of the program for future applications. A set of examples that are included as part of the software package downloaded are used for the certification and validity of the program, and they have been confirmed to provide accurate results (Buhl Jr. & Manjock, 2006). The Certification Test "Cer.Test" 12 was chosen because the turbine specifications such as hub height, rotor configuration are suitable for the Isabela site. The example has a rotor configuration of 3 blades with a diameter of 70 meters, a hub height of 84.3 meters and a rated power of 1.5 MW.

The wind condition for Cer.Test 12 is extreme coherent gust with direction (ECD) as described in the IEC standards section (International Electrotechnical Commission, 2005) section 6.3.2.5. The ECD is a sudden increase in wind speed due to a gust of wind accompanied by a change in the wind's direction. The horizontal wind speed behavior as presented by the IEC is formulated in equation 12. The initial conditions, before the beginning of the ECD event ($t \leq 0$), is as described by equation 2 once the event begins ($0 \leq t \leq T$) a gradual increase of the wind speed begins. When the time reaches the rise time T, the wind speed at set elevation will be the sum of the normal condition for the horizontal wind speed plus the full magnitude of the extreme coherent gust. To calculate the normal horizontal wind speed the IEC presents a wind shear coefficient of 0.11 or 0.20; depending on the turbine class (Class-S is not included). Figure A-2 presents the increase in wind speed over time as define by equation 10 and using an extreme coherent gust of 15 $m \cdot s^{-1}$, with a wind shear coefficient 0.2, rise time of 10 seconds, a hub height of 84.3 meters and a horizontal wind speed at hub height of 11.8 $m \cdot s^{-1}$, like in Cer.Test 12.

ECD - Horizontal wind speed

$$V(z,t) = \begin{cases} V(z) \ \ see\ Equation\ (2)\ , t \leq 0 \\ V(z) + \ 0.5 * V_{cg} * \left(1 - \cos\left(\frac{\pi * t}{T}\right)\right), 0 \leq t \leq T \\ V(z) + \ V_{cg}\ , t \geq 0 \end{cases} \quad (12)$$

where: T = rise time = 10 sec, and

V_{cg} = extreme coherent gust magnitude = 5 m·s^{-1}.

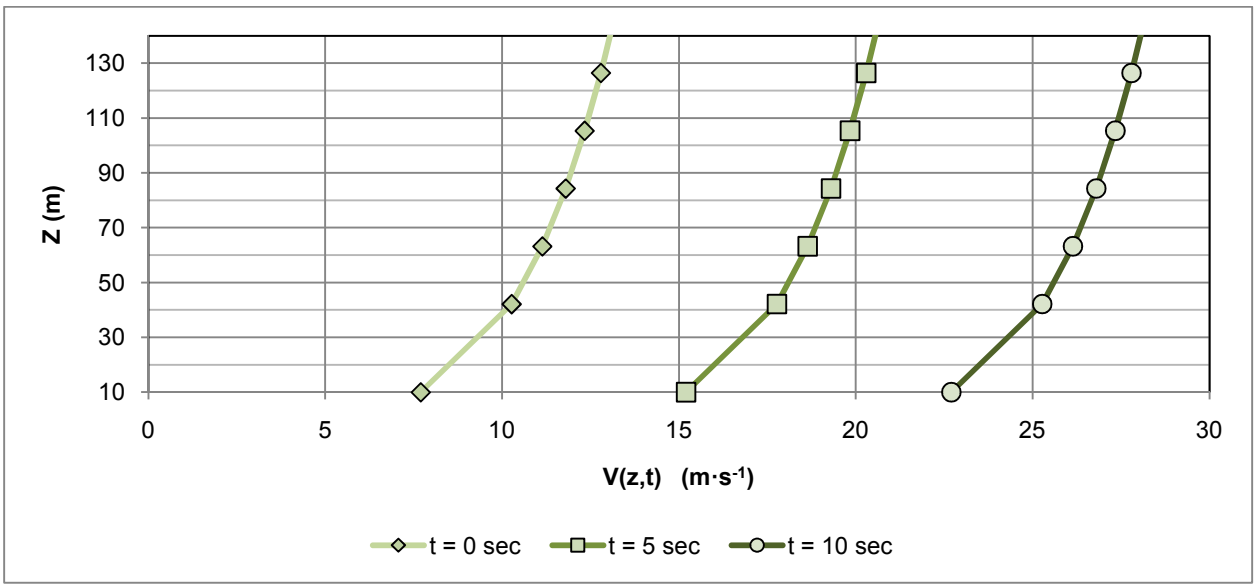

Figure A-2 : Effect of extreme coherent gust: α=0.2, T =10 sec, Z_{hub}=84.3m & V_{hub}=11.8m•s-1

The second component to the ECD event is a simultaneous direction change of the coherent gust. The magnitude of the direction change of the ECD is calculated with equation 13 and is reliant on the hub height horizontal wind speed. In Figure A-3, the behavior between the direction changes is presented. Wind speeds below 4 m·s^{-1} would have the same value of 180° and for values greater or equal to 4 m·s^{-1} it would have a lower magnitude angle that decreases in proportion to the increase in wind speed at hub height.

ECD - Horizontal wind direction for extreme coherent gust

$$\theta_{cg}(V_{hub}) = \begin{cases} 180°, & V_{hub} \leq 4\ m * s^{-1} \\ \dfrac{720°\ m * s^{-1}}{V_{hub}}, & 4\ m * s^{-1} \leq V_{hub} \leq V_{ref} \end{cases} \quad (13)$$

where : V_{ref} = Hub h reference wind speed as define in Table 1 of the IEC (International Electrotechnical Commission, 2005), and

V_{hub} = Hub height horizontal wind speed

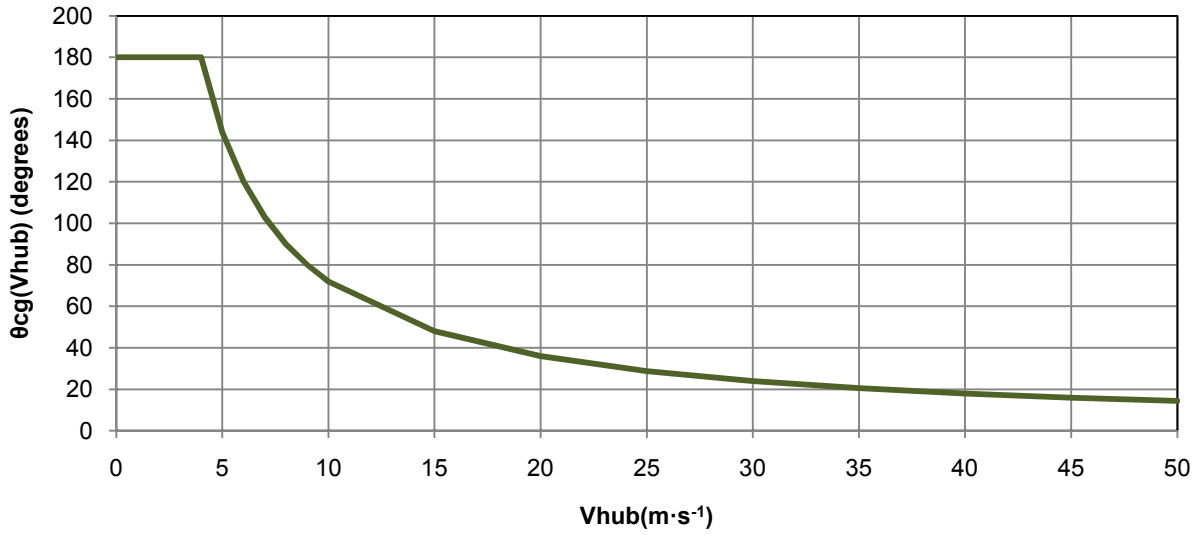

Figure A-3 : Magnitude of coherent gust change dependent on hub height wind speeds

The ECD the direction change does not occur instantaneously, but over the length of the rise time T. The progression of the change is defined in Equation 14 and is presented in Figure A-4. Initiating the transition at 0 degrees (perpendicular to the back of the rotor) the direction the progresses as t increases. The behavior is proportional to the increase in time as a cosine function of the time “t” and by “T”. When the rise time “T” is reached, the full magnitude of the direction change is achieved. It is essential to note that the direction change can be experienced for both negative and positive angles of orientation, which implies the possibility of the event originating from any lateral direction.

ECD - Horizontal wind direction

$$\theta(t) = \begin{cases} 0°, t \leq 0 \\ \pm 0.5 * \theta_{cg} * \left(1 - \cos\left(\frac{\pi * t}{T}\right)\right), 0 \leq t \leq T \\ \pm\theta_{cg}, t \geq 0 \end{cases} \qquad (14)$$

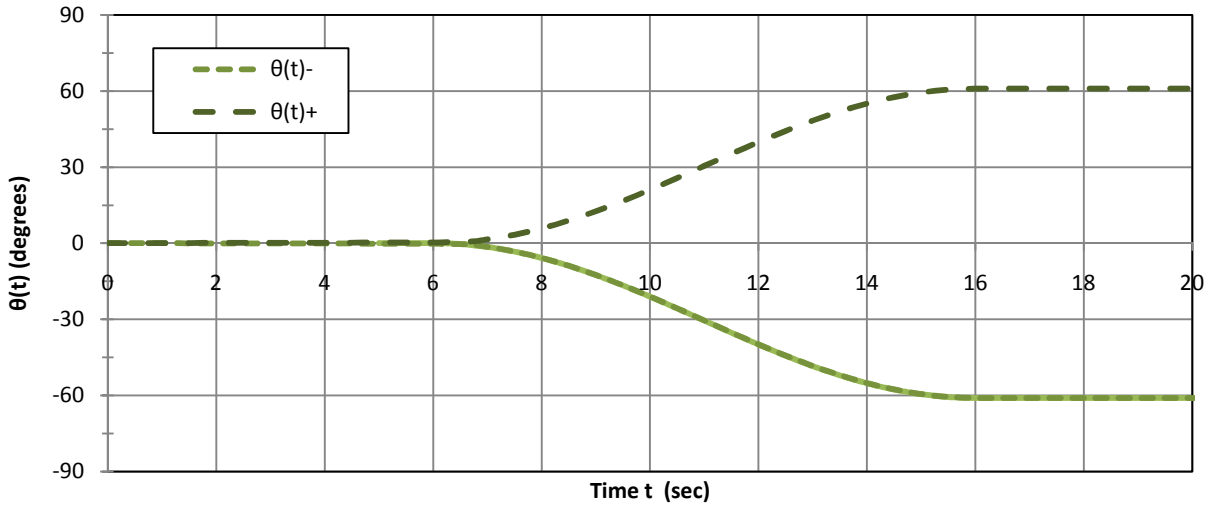

Figure A-4 : Direction change transition over time: T =10 sec, θcg=62.1 degrees

Using the parameters previously explained a wind file (extension .wnd) can be created to describe the wind conditions for the Cert.Test 12. Using the NREL codes *WindMaker* or *IECWind* the wind field conditions can be represented for the previously described case of EGD. Both programs require minimum information about the wind turbine like the class and hub height. Once the wind conditions are generated in the ".wnd file", it can be used and coupled with the structural information of the turbine, in the NREL codes (*AeroDyn* and *FAST*) to evaluate the behavior and response of the active turbine. The structural information requires knowledge of the nacelle, tower, blades and foundation dimensions and properties such as mass, inertia and stiffness. Once all the information has been supplied to the program, it generates a model of the turbine under the specified wind conditions. *Aerodyn* processes the

wind conditions as it relates to the turbine, and *FAST* resolves the equations of motion using a set of degrees of freedom defined by the program. The resulting information is presented in an output file (extension .out) and contains vectors of variables dependent on time as presented in the example in Figure 4-10. The resulting variables can be specified in the input file and can include the input wind characteristics (horizontal speed and direction), moments, forces and deflections for the turbine components along its local principal axis (X, Y & Z).

Figure A-5 and Table A-2 show the output parameters available for the tower base loads. The loads and moments act along their individual axis, green segmented lines, in Figure A-5 a) top view and b) a side view that presents the base section that connects to the bottom tower section for a wind turbine. The center circle in the top view indicates the tower base footprint, and on the side view the center lines at the top of the foundation are the foundation ring for the tower. The tower base loads are identified by having the initial TwBs fallowed by F for forces and M for moments, the last two letters indicate the axis in which the force is acting in addition for tower base loads it includes the letter t at the end, corresponding to the specific coordinate system for the tower loads.

Table A-2 : Tower base output load from FAST

Name	Description	Units	Direction
TwrBsFxt	Tower base force-at shear force	KN	along X-axis
TwrBsFyt	Tower base side-to-side shear force	KN	along Y-axis
TwrBsFzt	Tower base axial force	KN	along Z-axis
TwrBsMxt	Tower base roll (or side to side) moment, caused by side to side force	KN*m	about X-axis
TwrBsMyt	Tower base roll (or fore-aft) moment, caused by side to side force	KN*m	about Y-axis
TwrBsMzt	Tower base yaw moment, torsional	KN*m	about Z-axis

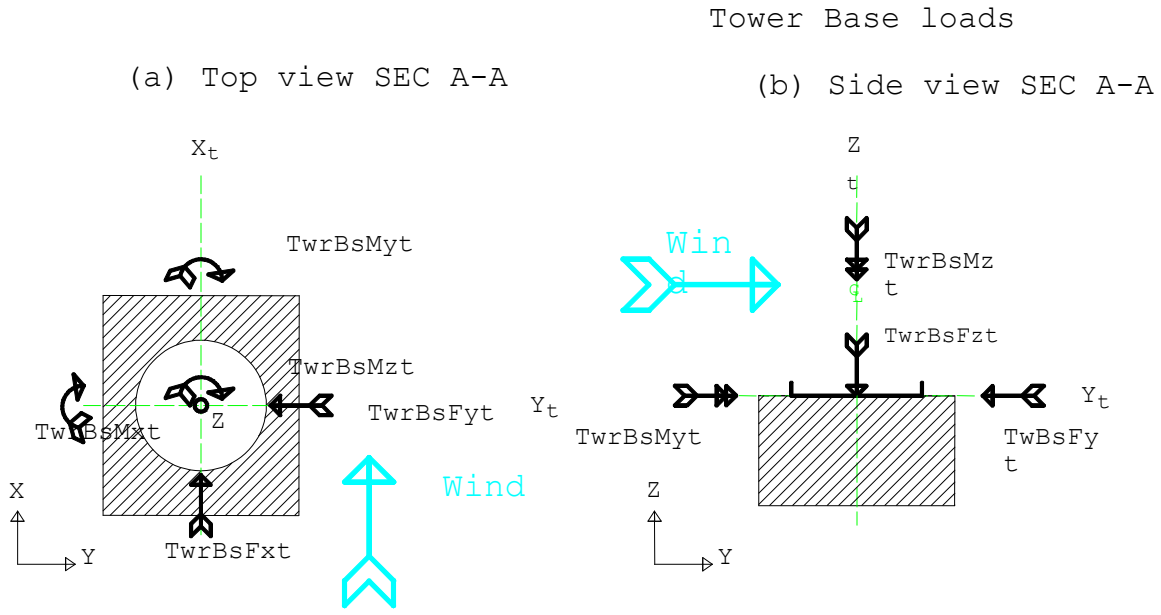

Figure A-5 : Output base loads from FAST a) top view and b) side view

Test 12 includes a pitch control program. The pitch control manages the angle of orientation of the turbine blades. Each blade is capable of rotating upon its center at the point where the blade and rotor meet (see Figure A-6). The pitch control can be used for several purposes such as to rotor acceleration control, energy output and load magnitude. It works by controlling the blade surface in the direction of the incoming wind. Figure A-6 a) displays the perpendicular orientation of the blade pitch. In this position the maximum area of the blades is in direct contact with the upcoming wind and should produce the maximum loads. In contrast, part b of the same figure displays the parallel position to the blades to the upcoming wind, for this position the loads should lower. The pitch control program was specifically designed for this Cert. Test by NREL. It remains constant at a low pitch angle for the initial time up to 7 seconds, it then begins to increase up until it reaches 17 degrees and then decreases until it levels off at around 10 degrees, and the pattern remains consistent for all three blades.

a) Perpendicular to wind

b) Parallel to wind

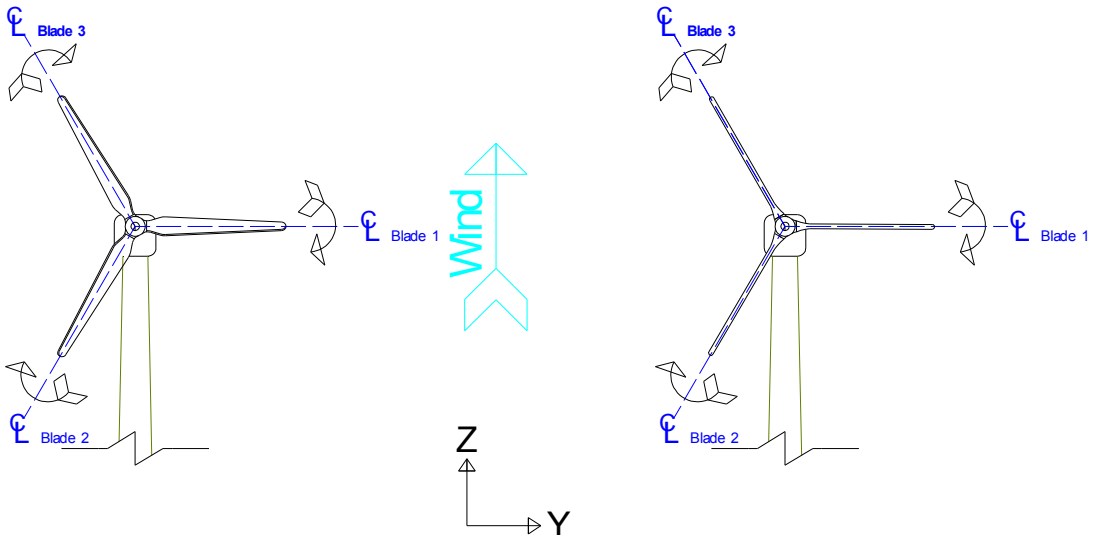

Figure A-6 : Blade pitch orientation variation a) Perpendicular and b) Parallel to wind

For Cert.Test 12, TwBsFyt and TwBsFyt are used as output parameters and are displayed in Figures A-7 and A-8. The figures present the individual forces (y-axis) as they act over time (x-axis) since the ECG begins, 5 seconds, until the rise time "T" is reached, 20 seconds. The behavior of both forces can be connected to the pitch control; whereas the pitch increases the magnitude of the resulting forces decreases. Consequently when comparing both forces as the direction changes (Figure A-4), the intensity of the forces move from the x_t to the y_t as expected because of the shift in direction. Continued oscillation of the loads can be accounted for by the continue motion of the rotor since the turbine is active during the event.

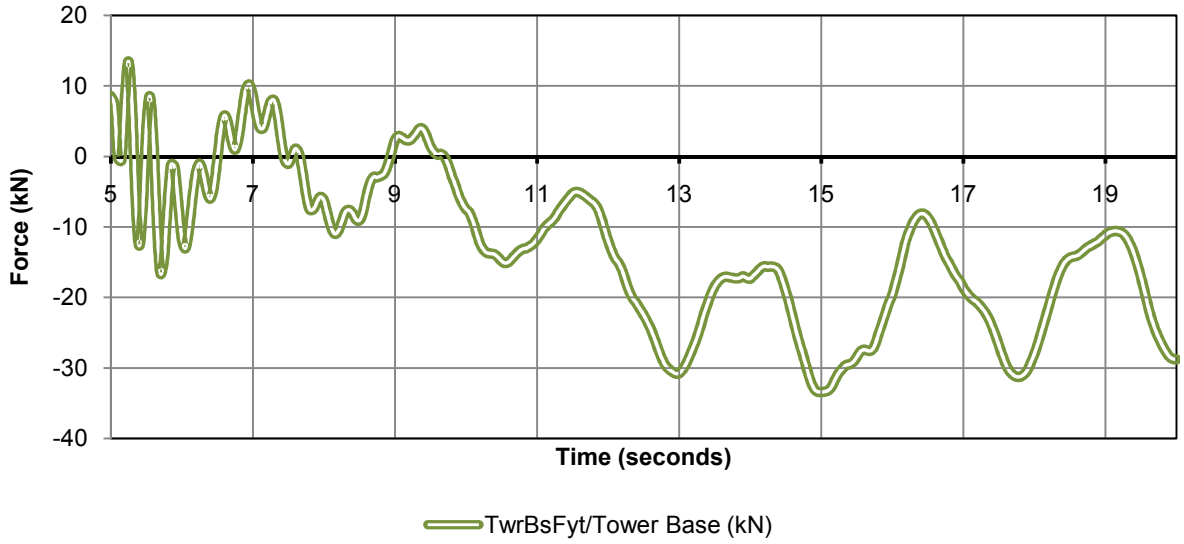

Figure A-7 : Wind turbine tower forces along-yt-axis for Cert.Test 12-Output

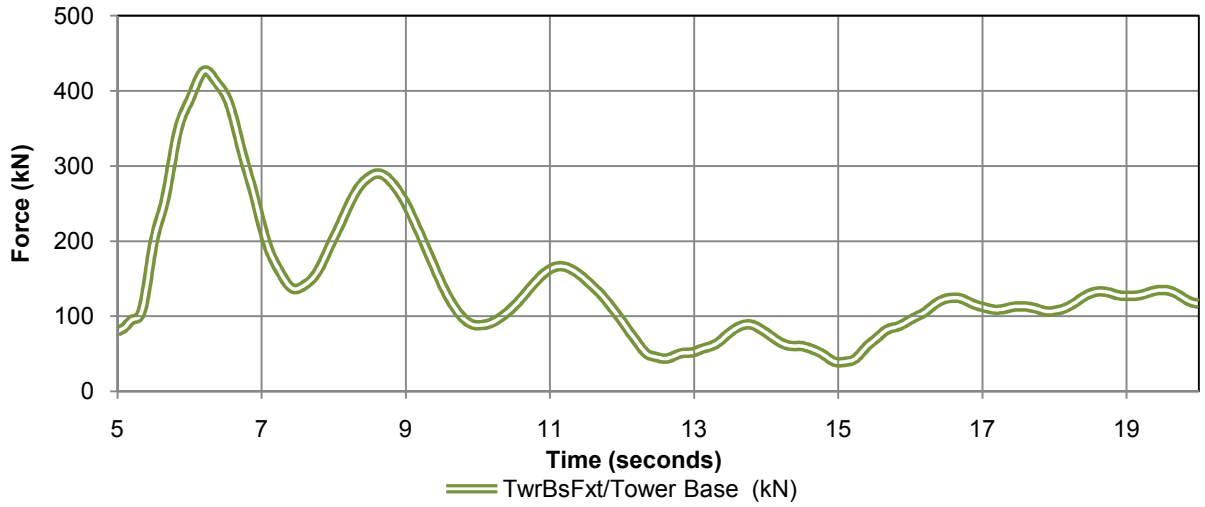

Figure A-8 : Wind turbine tower forces along-xt-axis for Cert.Test 12-Output